# MARS15 Overview

Nikolai Mokhov, Fermilab

Hadronic Shower Simulation Workshop
Fermilab
September 6-8, 2006

# OUTLINE

- Introduction
- Transported Particles and Energies
- Nuclear Cross Sections
- Inclusive Event Generators
- Exclusive Event Generators
- Muons, Neutrinos, Nuclear Capture, Annihilation
- Correlated Energy Loss and Coulomb Scattering
- Physics Process Bias Control and Tagging
- Geometry Options
- MAD-MARS Beam Line Builder
- Materials, Histograming, GUI, Multiprocessing
- A Couple of Recent Applications

# INTRODUCTION

The MARS code system is a set of Monte Carlo programs for detailed simulation of hadronic and electromagnetic cascades in an arbitrary 3-D geometry of shielding, accelerator, detector and spacecraft components with energy ranging from a fraction of an electronvolt up to 100 TeV. It has been developed since 1974 at IHEP, SSCL and Fermilab. The current MARS15 version combines the well established theoretical models for strong, weak and electromagnetic interactions of hadrons, heavy ions and leptons with a system which can contain up to $10^5$ objects, ranging in dimensions from microns to hundreds kilometers. A setup can be made of up to 100 composite materials, with arbitrary 3-D magnetic and electric fields. Powerful user-friendly GUI is used for visualization of geometry, materials, fields, particle trajectories and results of calculations. MARS15 has 5 geometry options and flexible histograming options, can use as an input MAD optics files through a powerful MAD-MARS Beam Line Builder, and provides an MPI-based multiprocessing option, with various tagging, biasing and other variance reduction techniques.

# Current Developers

Many people participated in the MARS code development over its 32-year history.

***Current contributors are:***

N.V. Mokhov, S.I. Striganov, K.K. Gudima, C.C. James, M.A. Kostin, S.G. Mashnik, M.E. Monville, N. Nakao, I.L. Rakhno, A.J. Sierk

Plus invaluable feedback from 300 MARS users worldwide

# TRANSPORTED PARTICLES AND ENERGIES

All important elementary particles with their corresponding decay modes are transported in the code. Arbitrary heavy ions with atomic mass $A$ and charge $Z$ are fully treated by MARS15. Their ID are coded as $ID = 1000Z + A - Z$.

| Nucleons & Mesons | Gauge & Leptons | Hyperons |
|---|---|---|
| $p\ \overline{p}$ | $\gamma$ | $\Lambda\ \overline{\Lambda}$ |
| $n\ \overline{n}$ | $e^+\ e^-$ | $\Sigma^+\ \overline{\Sigma}^+$ |
| $\pi^+\ \pi^-\ \pi^0$ | $\mu^+\ \mu^-$ | $\Sigma^0\ \overline{\Sigma}^0$ |
| $K^+\ K^-$ | $\nu_e\ \overline{\nu}_e$ | $\Sigma^-\ \overline{\Sigma}^-$ |
| $K^0\ \overline{K}^0$ | $\nu_\mu\ \overline{\nu}_\mu$ | $\Xi^0\ \overline{\Xi}^0$ |
| $K_L^0\ K_S^0$ | | $\Xi^-\ \overline{\Xi}^-$ |
| | | $\Omega^-\ \overline{\Omega}^-$ |

Hyperon production is possible only in the exclusive mode or from a pre-generated source.

Maximum energy 100 TeV. Cutoff energies: 0.001 eV neutrons, 100 keV electrons and photons, and about 10 keV others.

# NUCLEAR CROSS SECTIONS

Total and elastic cross sections of hadron-nucleon interactions for ordinary hadrons are described using corresponding fits to experimental data. X-sections for hyperon-nucleon interactions are described via the ordinary hadron x-sections using the Additive Quark Model rules. At energies above 5 GeV, such an approach agrees well with data. At lower energies, the hyperon-nucleon x-sections are very close to proton-nucleon ones. Hadron-nucleus total and inelastic x-sections at energies above 5 GeV are calculated using the Glauber model. At lower energies, parameterizations to experimental data are used. For neutral kaons, cross sections on both nucleon and nucleus targets are calculated using the relation based on isospin and hypercharge conjugation. Total and inelastic x-sections for heavy-ion nuclear interactions are based on the JINR model.

# PION AND ANTIPROTON X-SECTIONS ON PROTON

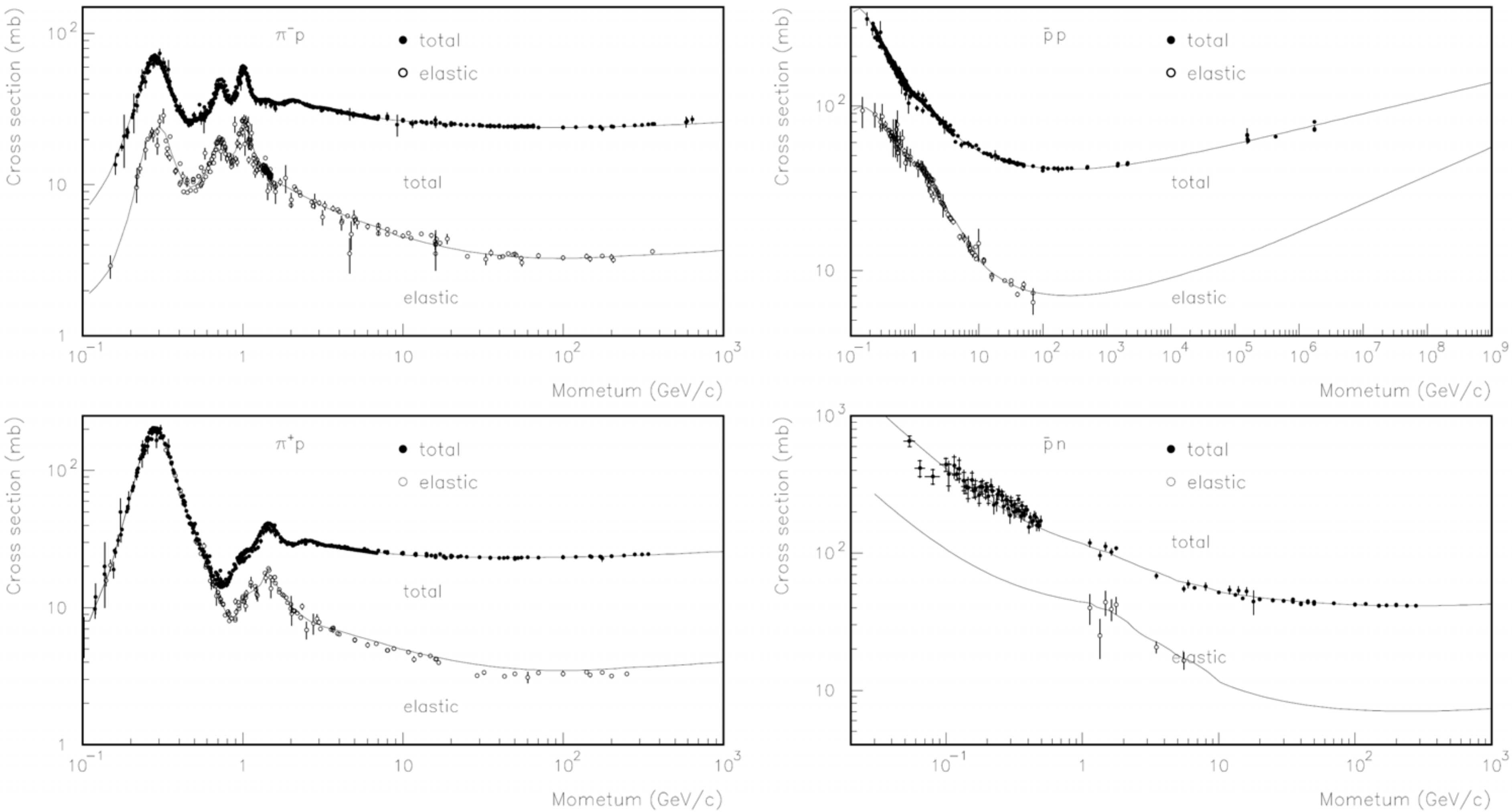

# KAON AND HYPERON X-SECTIONS ON PROTON

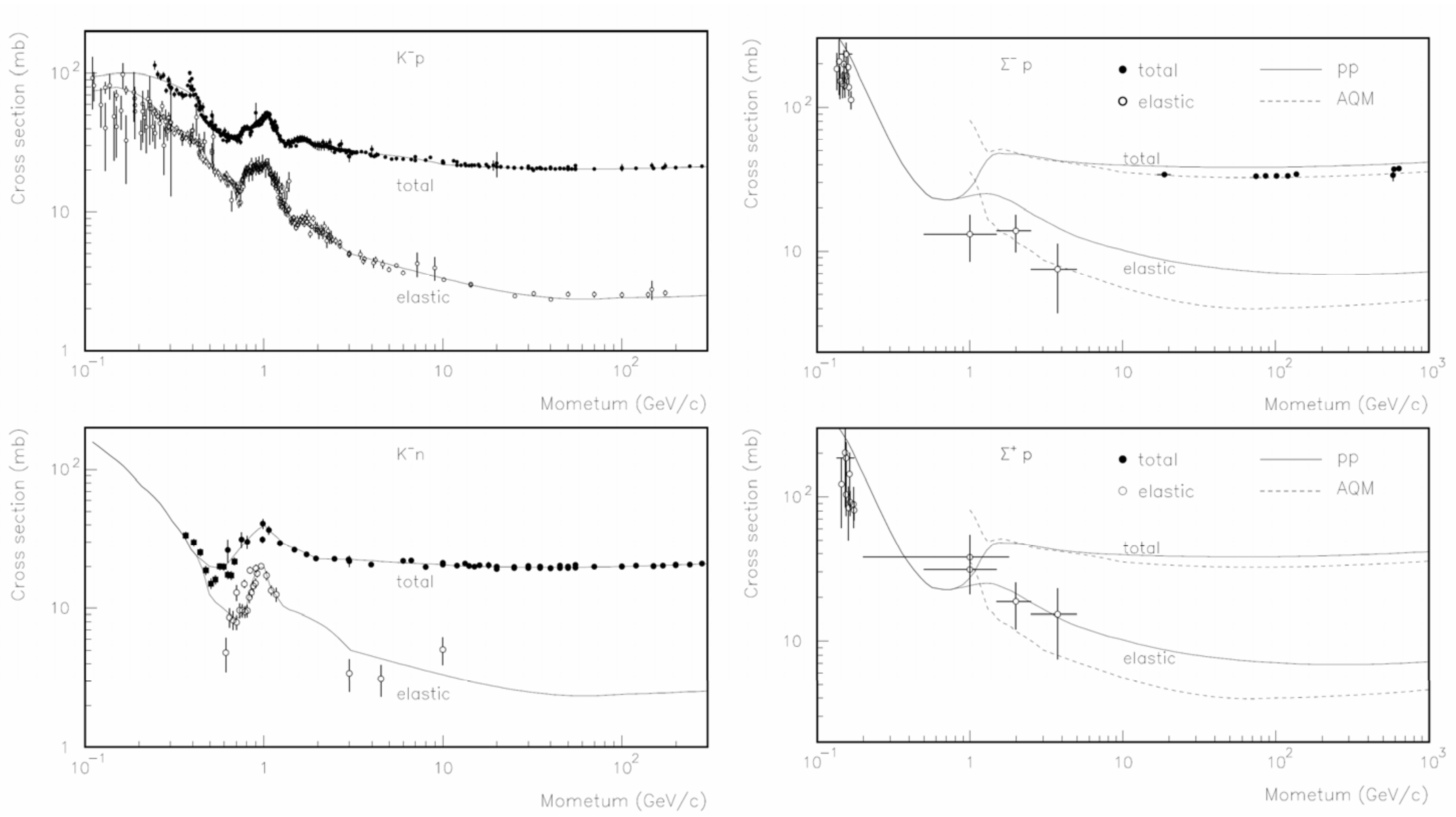

# NEUTRONS AND ANTI-NEUTRONS ON NUCLEI

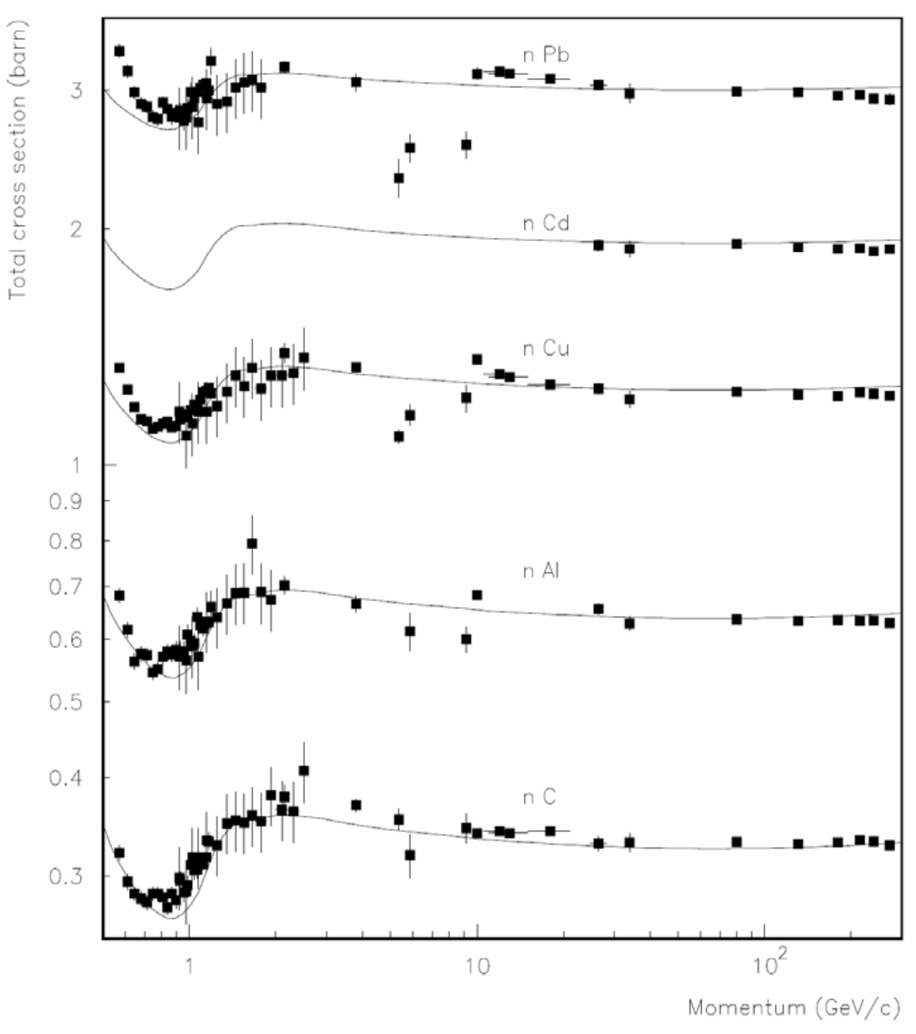


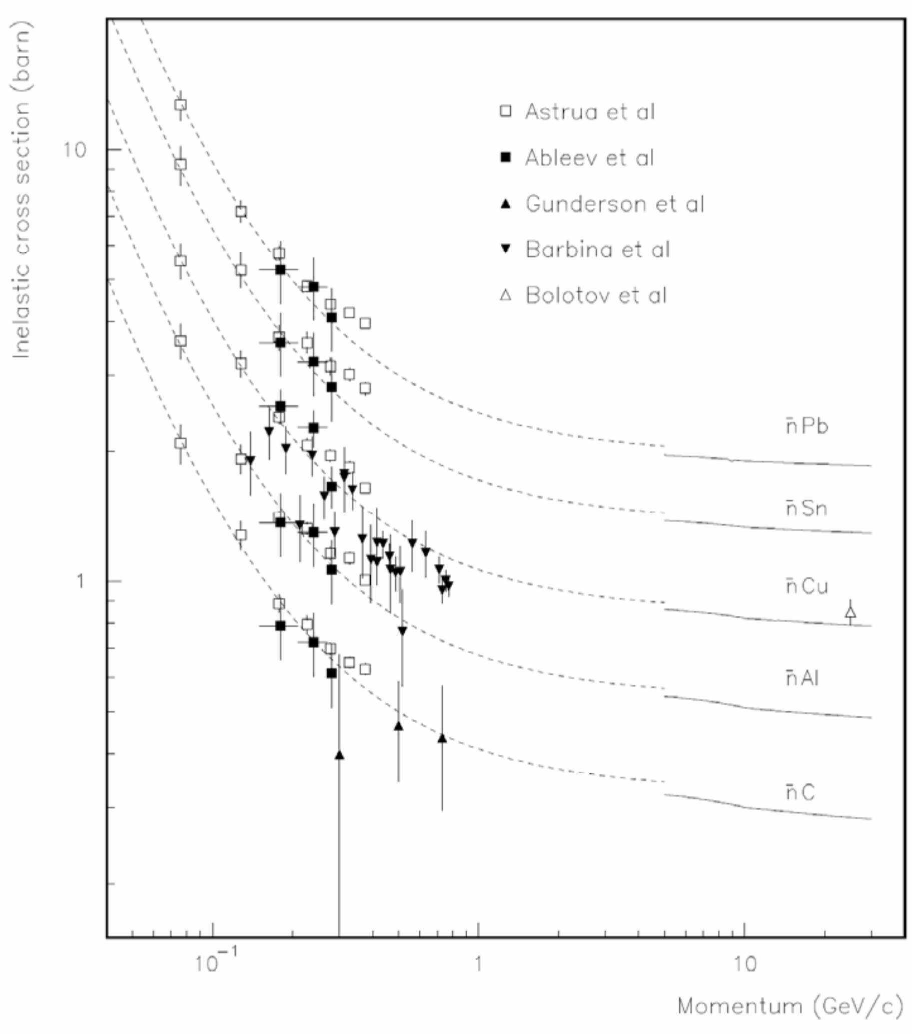

# NUCLEUS-NUCLEUS X-SECTIONS

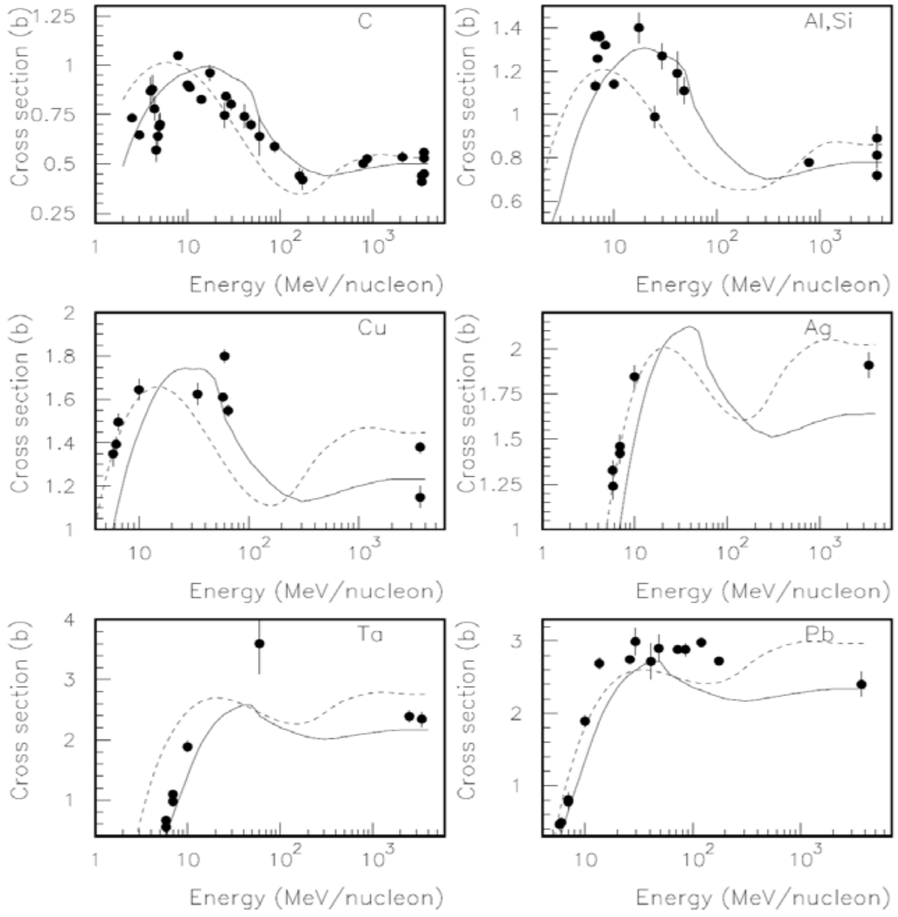


$^{4}$He–nucleus reaction cross section

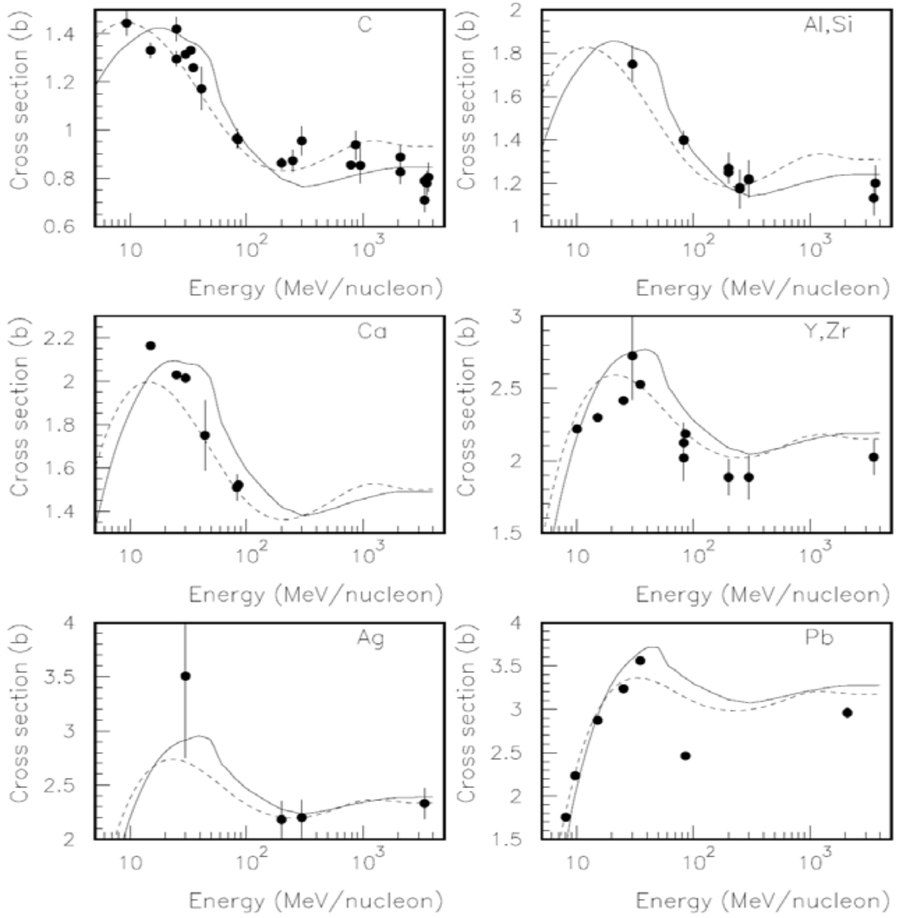


$^{12}$C–nucleus reaction cross section

Inelastic x-sections for 4He (left) and 12C (right) ions on various nuclei according to JINR (solid, used in MARS15) and NASA (dashed) models

# MARS INCLUSIVE APPROACH (1)

The basic model for the original MARS program, introduced in 1974, came from Feynman's ideas concerning an inclusive approach to multiparticle reactions and *weighting* techniques. At each interaction vertex, a particle cascade tree can be constructed using only a fixed number of representative particles (the precise number and type depending on the specifics of the interaction), and each particle carries a statistical weight $w = f(x)/S(x)$, which is equal, in the simplest case, to the partial mean multiplicity of the particular event. Energy and momentum are conserved *on average* over a number of collisions. It was proved rigorously that such an estimate of the first moment of the distribution function $f(x)$ is unbiased.

# MARS INCLUSIVE APPROACH (2)

The practical reasons for the inclusive scheme are:

- the CPU time per incident particle grows only logarithmically with incident energy, compared to the linear rise in the exclusive mode, and this allows for easier simulation of multi-TeV particle cascades;
- in many applications one considers effects due to the simultaneous interactions of a huge number of particles, so to describe the cascades it is sufficient to obtain the first moment of the distribution function using the inclusive cross-sections, in the same manner as with Boltzman's equation;
- experimental data on inclusive interaction spectra are more readily available than for exclusive ones;
- the use of statistical weights allows the production of a given particle type to be enhanced within the phase-space region of interest, especially for rarely produced particles.

# MARS INCLUSIVE HADRON-NUCLEUS VERTEX

It was found that the following biasing scheme for hA vertex provides the highest efficiency $\varepsilon = (t\sigma^2)^{-1}$ in detector, accelerator and shielding applications:

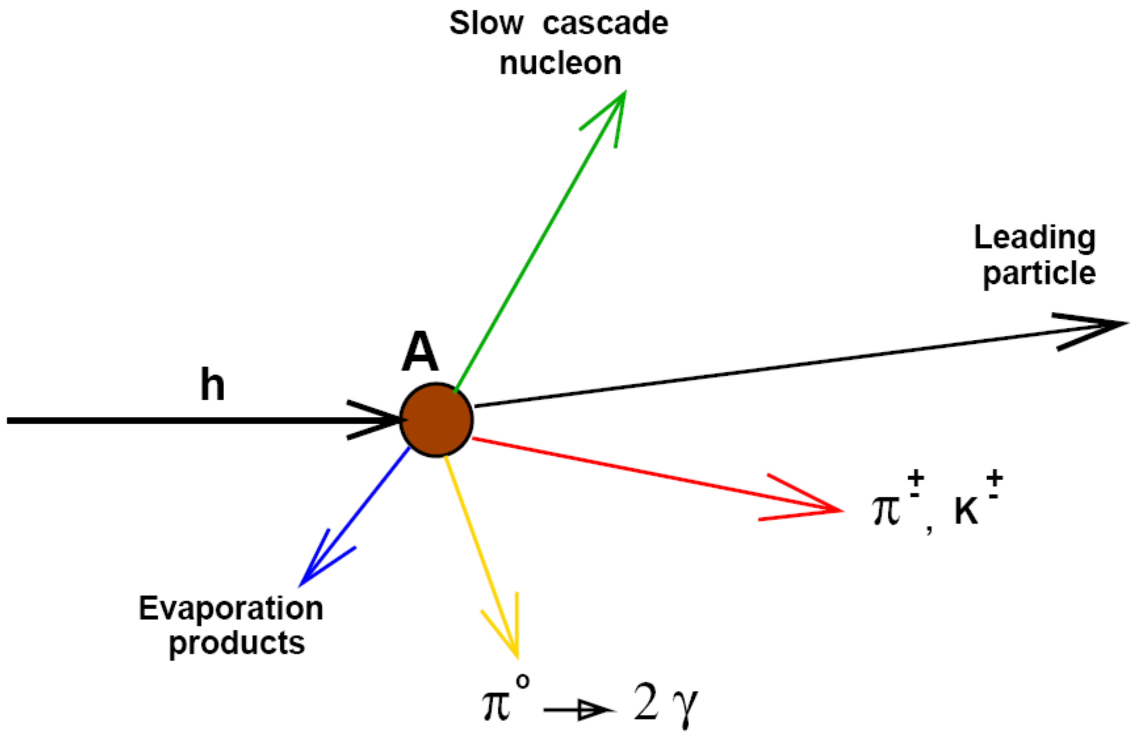

# Hadron Vertex: Exclusive and Inclusive

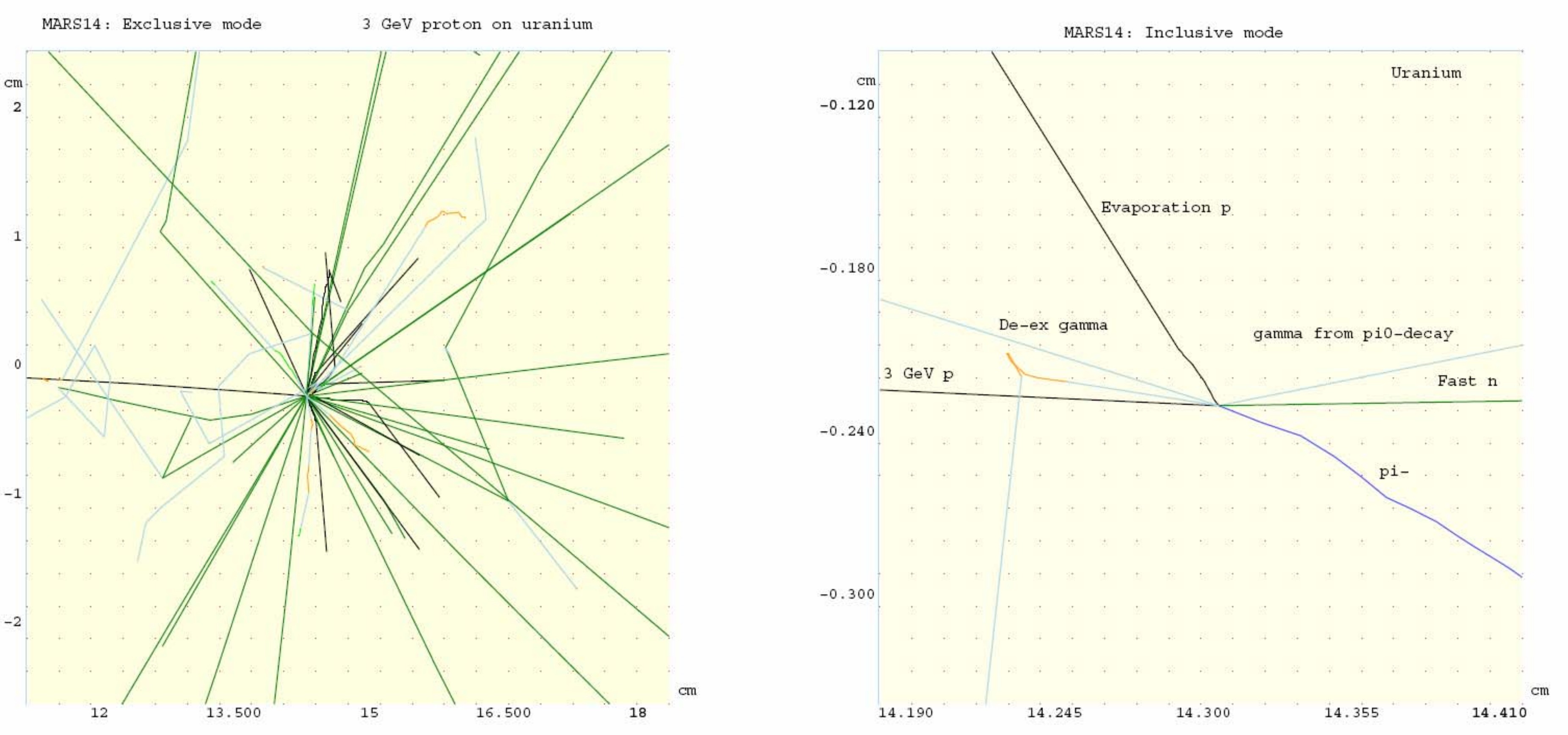


3-GeV proton on 20-cm uranium target

# EMS Exclusive and Inclusive

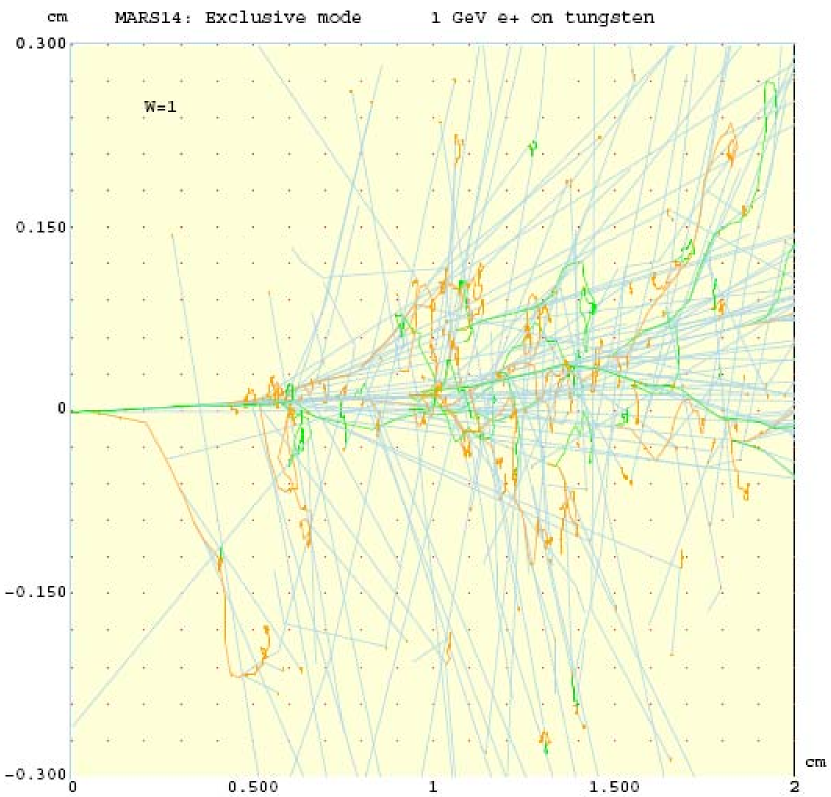


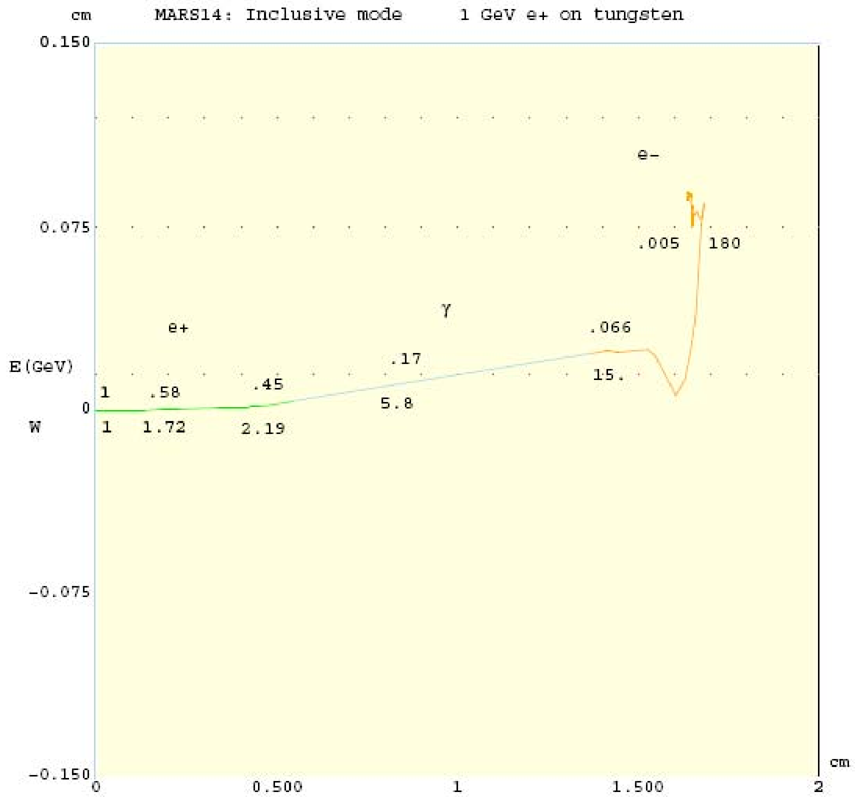


1-GeV positron on 2-cm tungsten target

# INCLUSIVE NUCLEON PRODUCTION

Two-year developments of a new phenomenological model of nucleon production in hadron-nucleus interactions above a few GeV have been completed in 2005. Proton inclusive spectra in pp-interactions are described:

- in resonance region $x_F > 1\text{-}2.2/p_0$ as a sum of five Breit-Wigner resonances;
- in diffractive dissociation region $1\text{-}2.2/p_0 < x_F < 0.9$ via triple-Reggeon formalism;
- in fragmentation region $0.4 < x_F < 0.9$ via phenomenological model with a flat behavior on longitudinal and exponential on transverse momenta;
- in central region $0 < x_F < 0.4$ via fit to experimental data.

For pA, it is factorized then with R(A,p,p0) function adjusted with additive quark model, with quasielastic scattering and Fermi-motion modeled in addition, supplied with a phenomenological model for cascade and evaporation nucleon production.

**Combined with new anti-nucleon production and fission models.**

# INCLUSIVE PROTON PRODUCTION

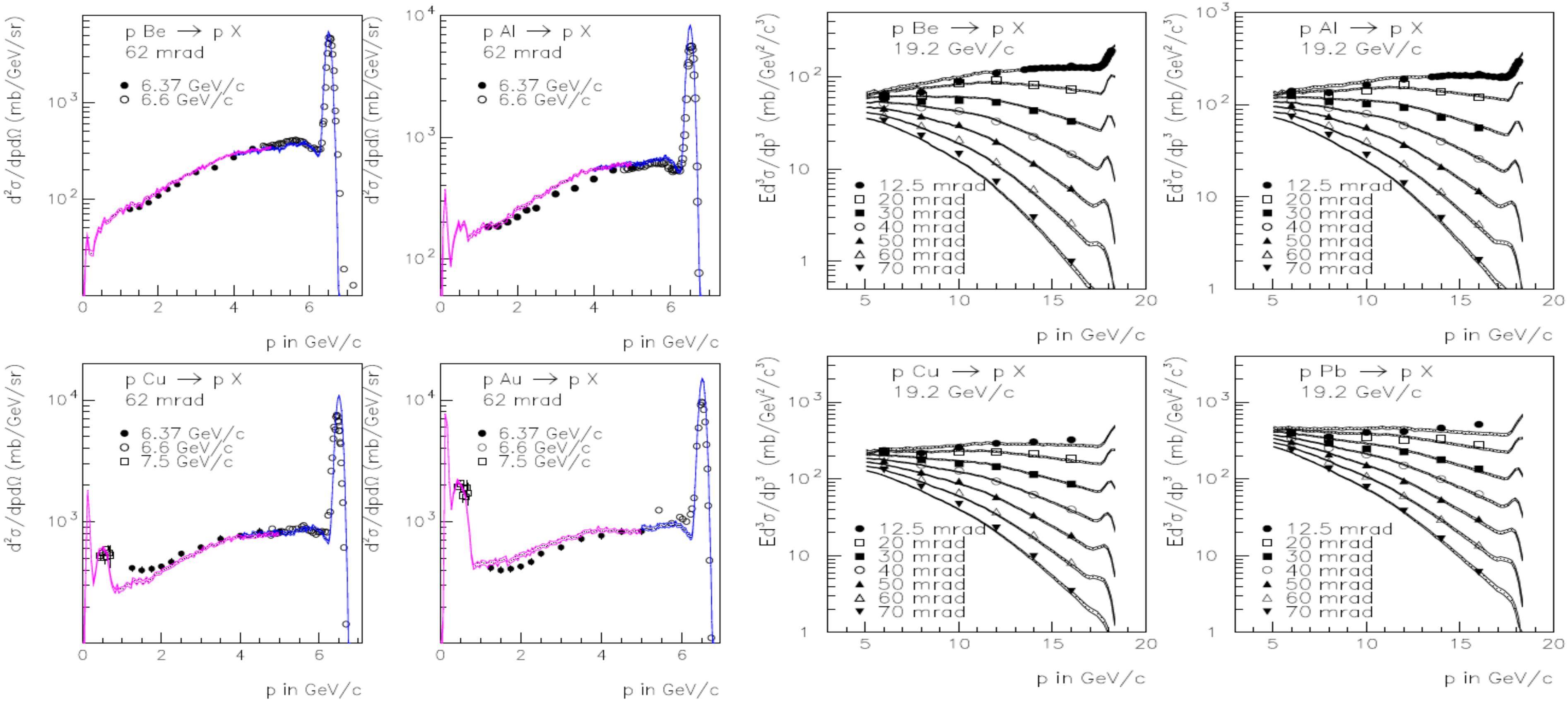

# PROTON AND PBAR PRODUCTION

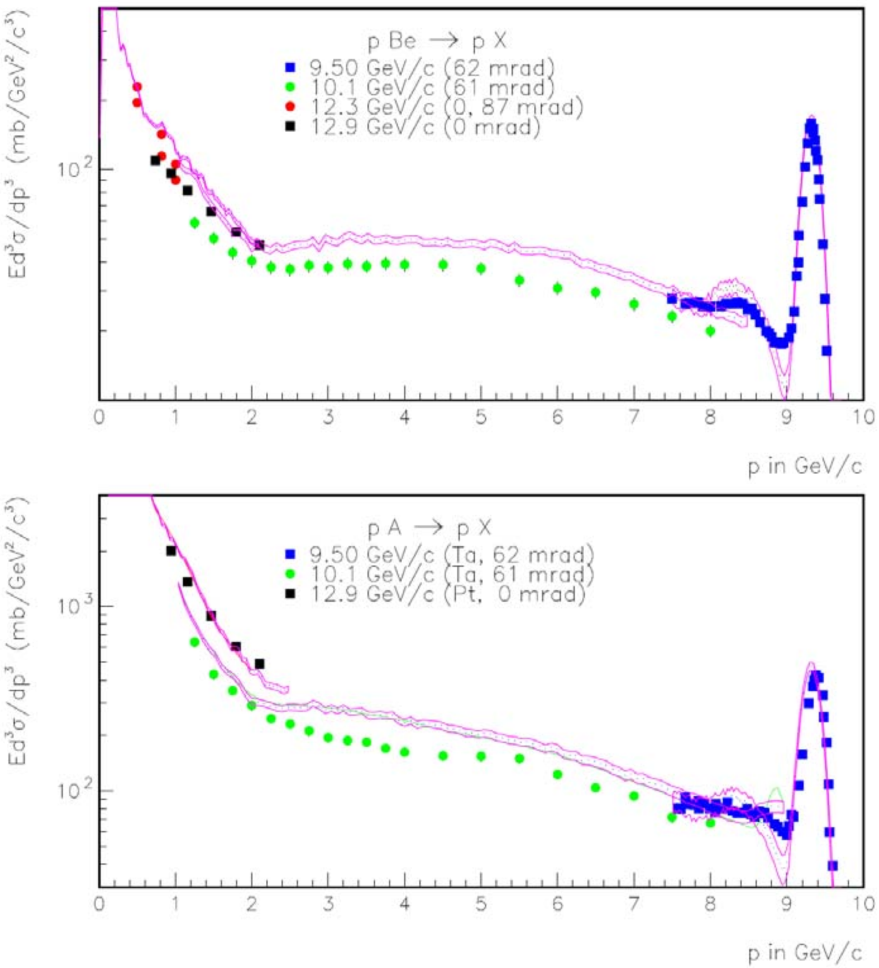


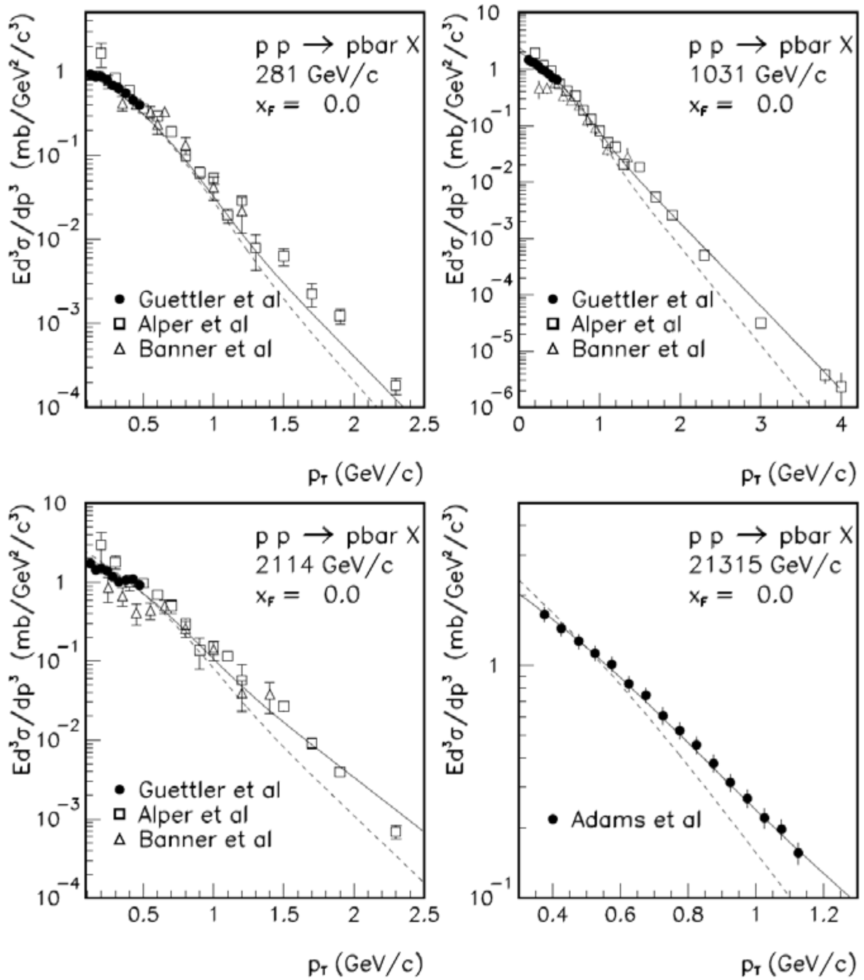

# Meson Production Model (1)

The inclusive MARS model of pion/kaon production is based on the following factorization

$$\frac{d^2\sigma^{pA\to\pi^\pm X}}{dpd\Omega} = R^{pA\to\pi^\pm X}(A, E_0, p, p_\perp)\frac{d^2\sigma^{pp\to\pi^\pm X}}{dpd\Omega},$$

where $E_0$ – proton energy, $p$ and $p_\perp$ – total and transverse momentum of $\pi^\pm$.

Atomic mass dependence of pion production at $x_F > 0.05$ is is convenient to describe as $A^\alpha$. For proton with energy $\geq$ 70 GeV

$$\alpha_g = 0.8 - 0.75 * x_F + .45 * x_F^3/|x_F| + 0.1 * p_\perp^2$$

For $p_0 \geq 24$ GeV/c energy dependence is very weak. For lower momentum $\alpha$ can be approximated as

$$\alpha = \alpha_g - 0.0087 \cdot (24 - p_0)$$

# Meson Production Model (2)

Experimental data at $x_F < 0.05$ are sparse. We have found that scaling in form similar to proposed by Stenlund and Otterlund is valid

$$\frac{dN}{dY} = \frac{<N>}{Y_0} \cdot F(A, \frac{Y}{Y_0}),$$

where $<N>$ is mean multiplicity of $\pi^-$, $Y_0$ - rapidity of primary proton and $Y$ - rapidity of $\pi^-$. Scaling function can be fitted as

$$F(A, \frac{Y}{Y_0}) = c_1 \cdot exp(-(\frac{Y}{Y_0} - c_2)^2 / c_3).$$

Experimental data on rapidity distribution of $\pi^+$,$\pi^-$ in proton-proton interaction can be described as

$$\frac{dN}{dY} = C_{pp} \cdot exp(-\frac{Y_{cm}^2}{2\sigma^2}),$$

where $Y_{cm}$ is pion rapidity in center of mass system,

# INCLUSIVE MESON PRODUCTION

Phenomenological model of meson production above a few GeV has also been improved and extended to neutral kaons.

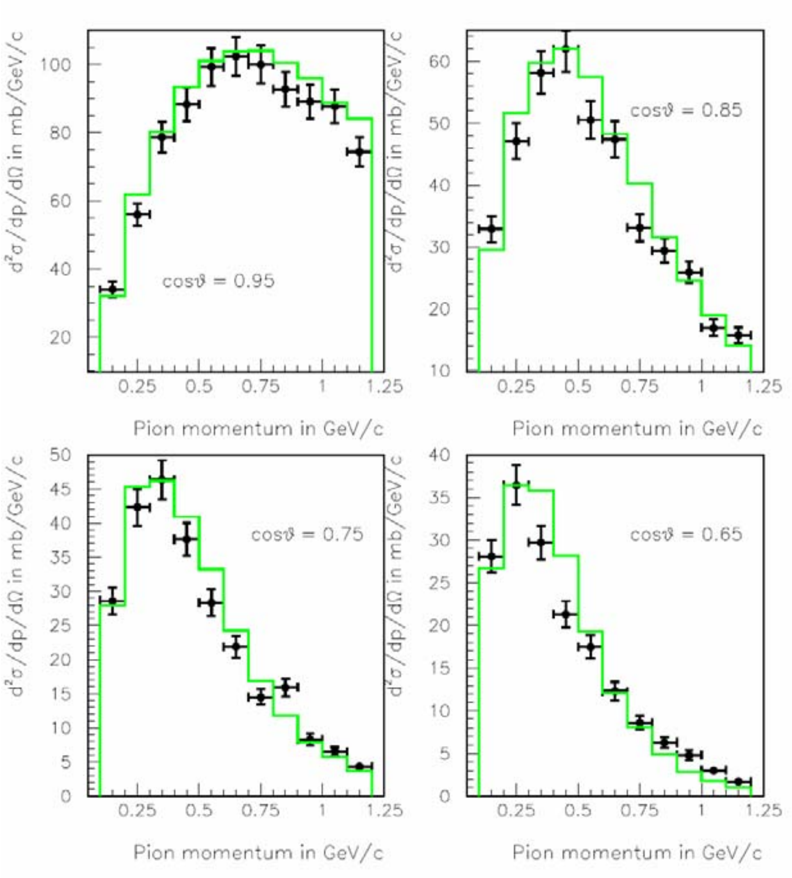


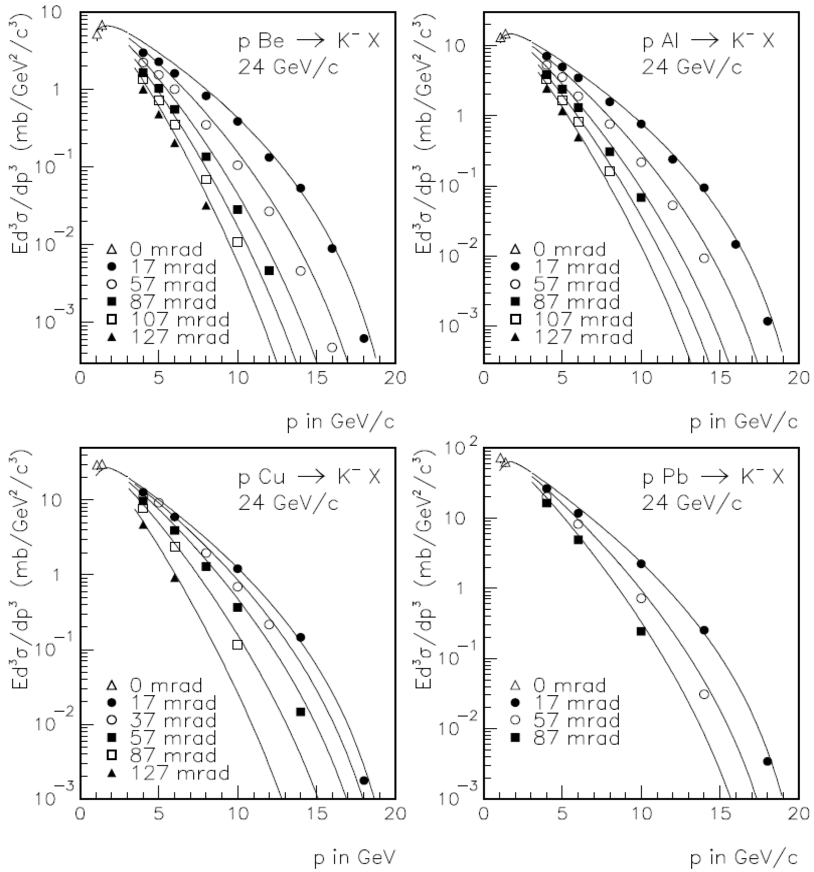


12.3 GeV/c p+Be -> $\pi^-$ vs BNL E910

# $K^-$ and $K_s$ Production

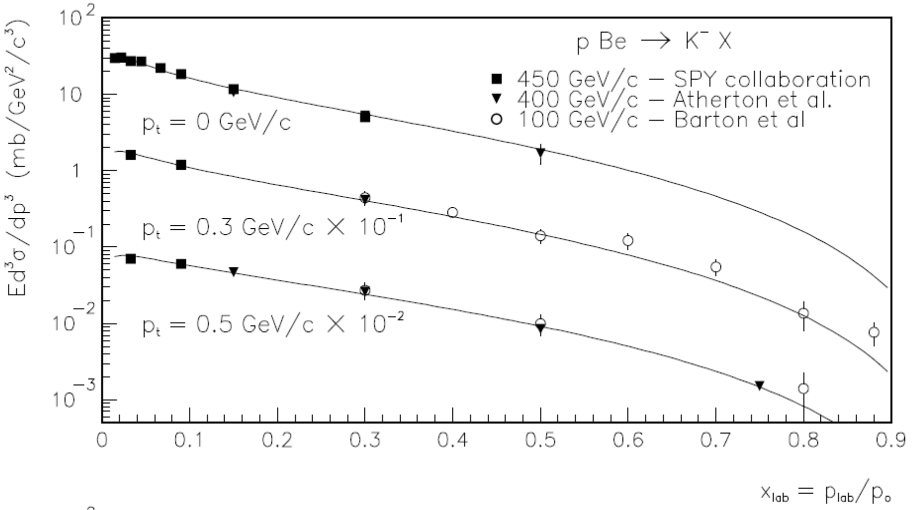


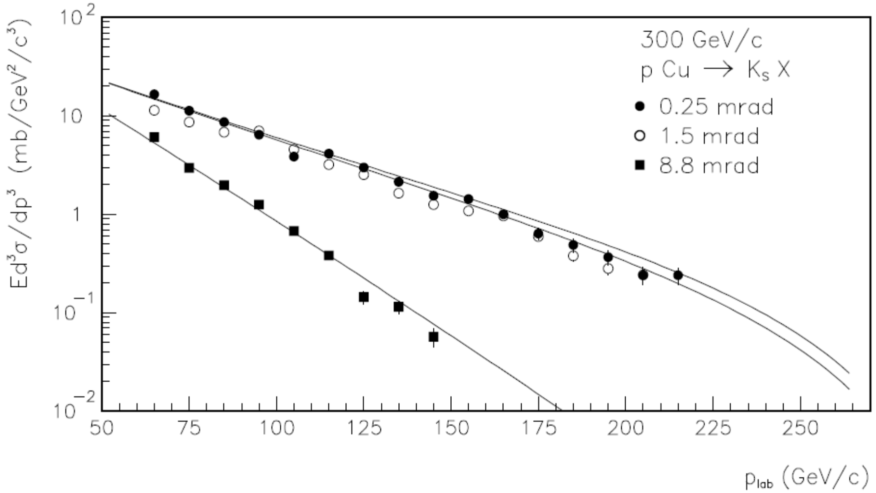


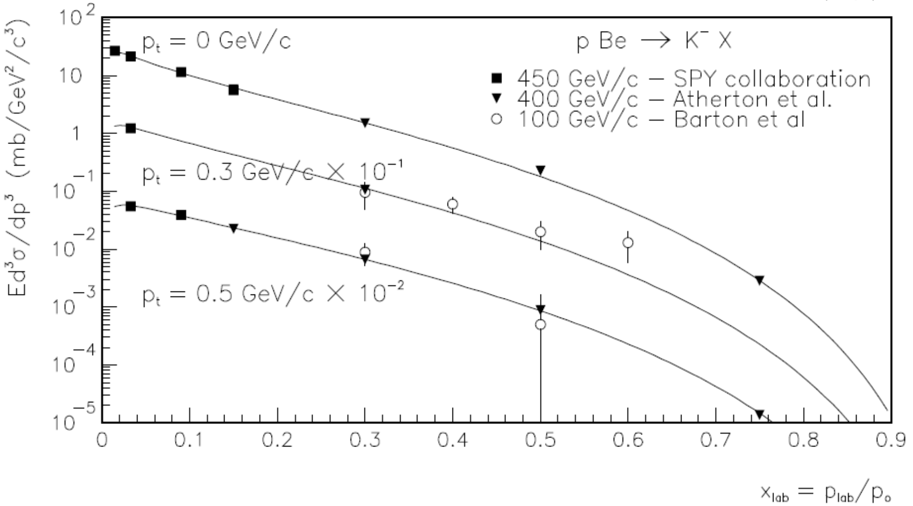


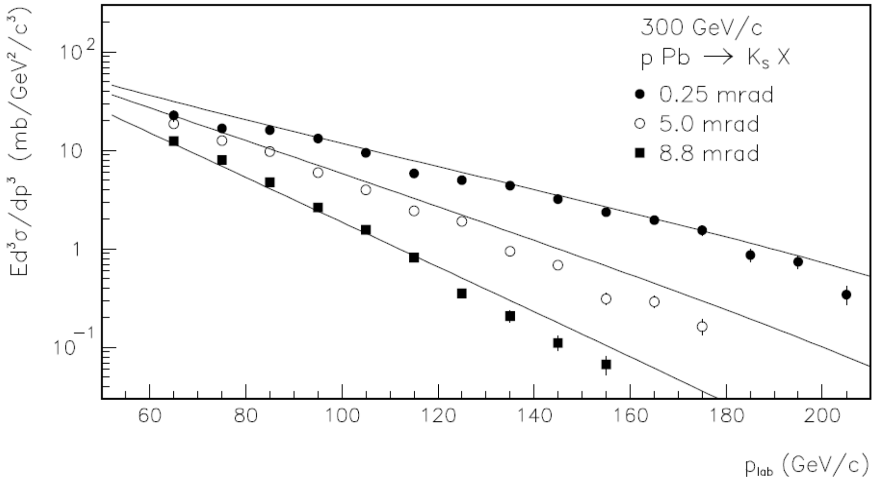


300 GeV/c p+Cu, Pb -> $K_s$

# MARS15 EXCLUSIVE EVENT GENERATORS

Substantially improved Cascade-Exciton Model code, **CEM03.01**, combined with the Fermi break-up model, the coalescence model, and an improved version of the Generalized Evaporation-fission Model (GEM2) is used as a default for hadron-nucleus interactions below 5 GeV. Recent multi-fragmentation extension.

The Los Alamos Quark-Gluon String Model code, **LAQGSM03**, was implemented into MARS15 for particle and heavy-ion projectiles at 10 MeV/A to 800 GeV/A. This provides a power of full theoretically consistent modeling of exclusive and inclusive distributions of secondary particles, spallation, fission, and fragmentation products. Further development of this package is underway.

For quite some time, MARS has used the Dual-Parton Model code, **DPMJET3**,for the very first vertex in a cascade tree. This is used in our numerous studies for the LHC 7x7 TeV collider and its detectors, and at very high energies up to 100 TeV.

# CEM03.01

CEM03.01 is the latest modification of the improved Cascade-Exciton Model (CEM). It is a completely new, updated, and modified version in comparison with its predecessors, not just an incremantal improvement.

**S. G. Mashnik, K. K. Gudima, A. J. Sierk, M. I. Baznat, N. V. Mokhov, "CEM03.01 User Manual", LANL LA-UR-05-7321 (2005)**

CEM03.01 describes reactions induced by nucleons, pions, and photons as a three-stage process: IntraNuclear Cascade (INC), followed by preequilibrium emission of particles during the deexcitation of the excited residual nuclei formed during the INC, followed by evaporation of particles from or fission of the compound nuclei. If the excited residual nucleus produced after the INC has a mass number $A < 13$, CEM03.01 uses a recently updated and improved version of the Fermi Break-up model to calculate its decay instead of considering a preequilibrium stage followed by evaporation from compound nuclei. CEM03.01 considers also coalescence of complex particles up to He-4 from energetic nucleons emitted during the INC.

# NUCLEON YIELDS in 0.56 and 8 GeV/A REACTIONS

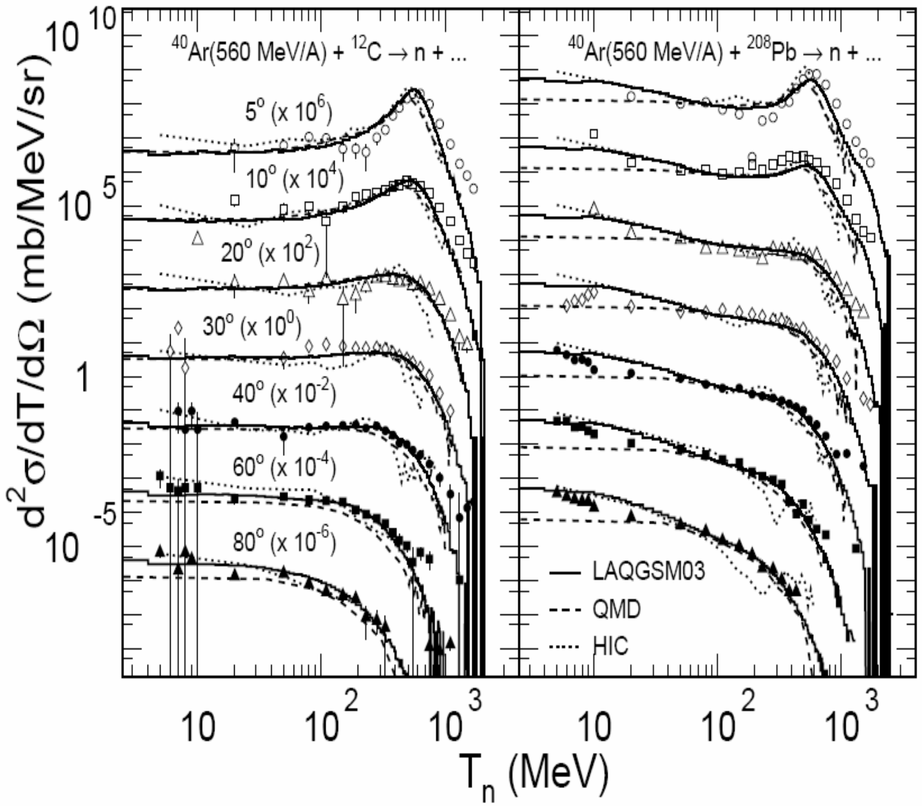


**FIGURE 3.** Differential cross-sections of neutrons in 560 MeV/A $Ar+C$ and $Ar+Pb$ reactions as calculated with LAQGSM03, JQMD [12] and HIC [13] codes *vs* data [14].

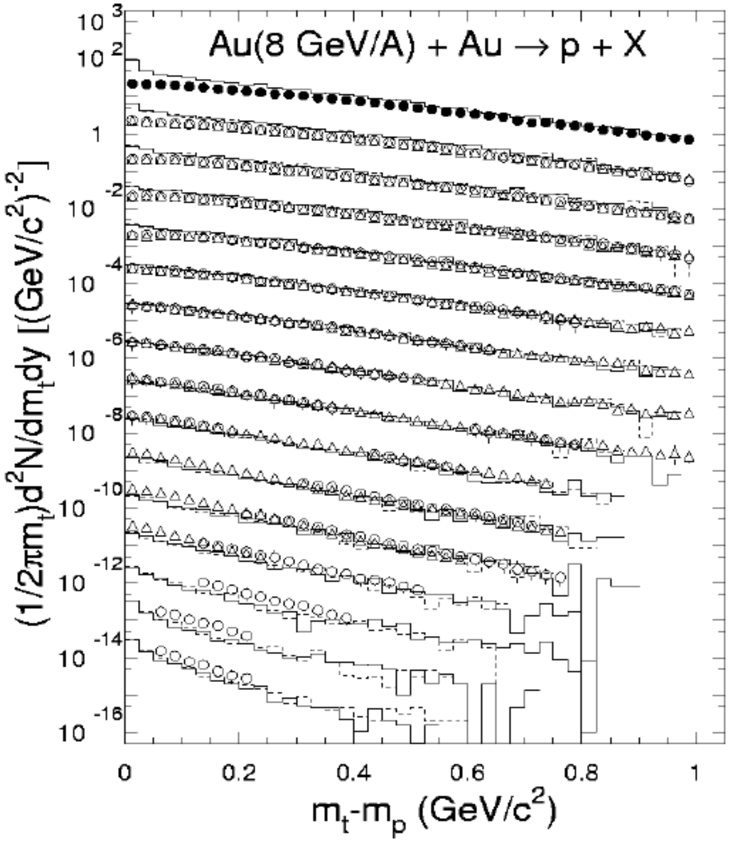


Figure 4. Invariant proton yield per central *Au+Au* collision at 8 GeV/A as calculated with LAQGSM03 (histograms) and measured in Ref. (12) (symbols). Solid lines and open circles is forward production, dashed lines and open triangles is backward production. Midrapidity (upper set) is shown unscaled, while the 0.1 unit rapidity slices are scaled down by successive factors of 10.

# NUCLIDE PRODUCTION AND PION SPECTRA FOR AA

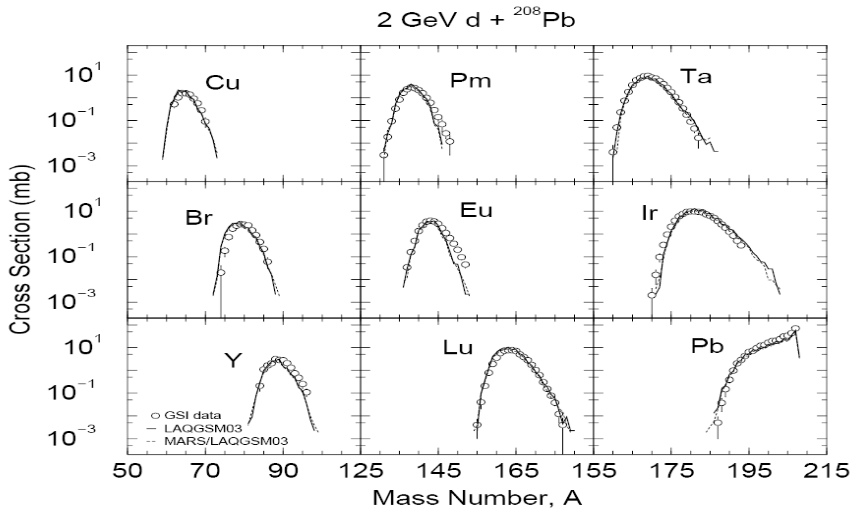


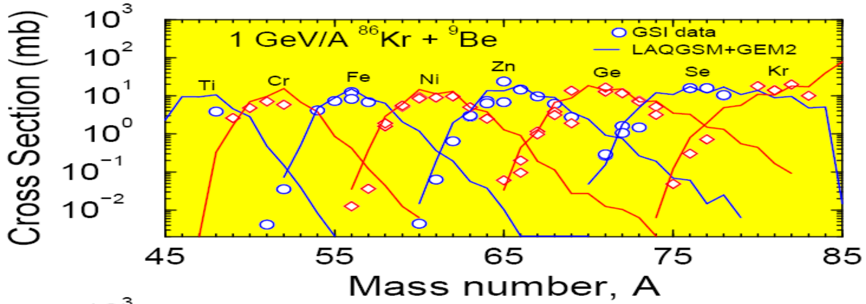


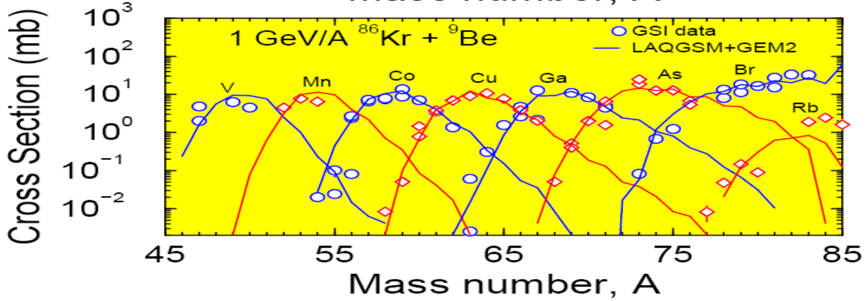


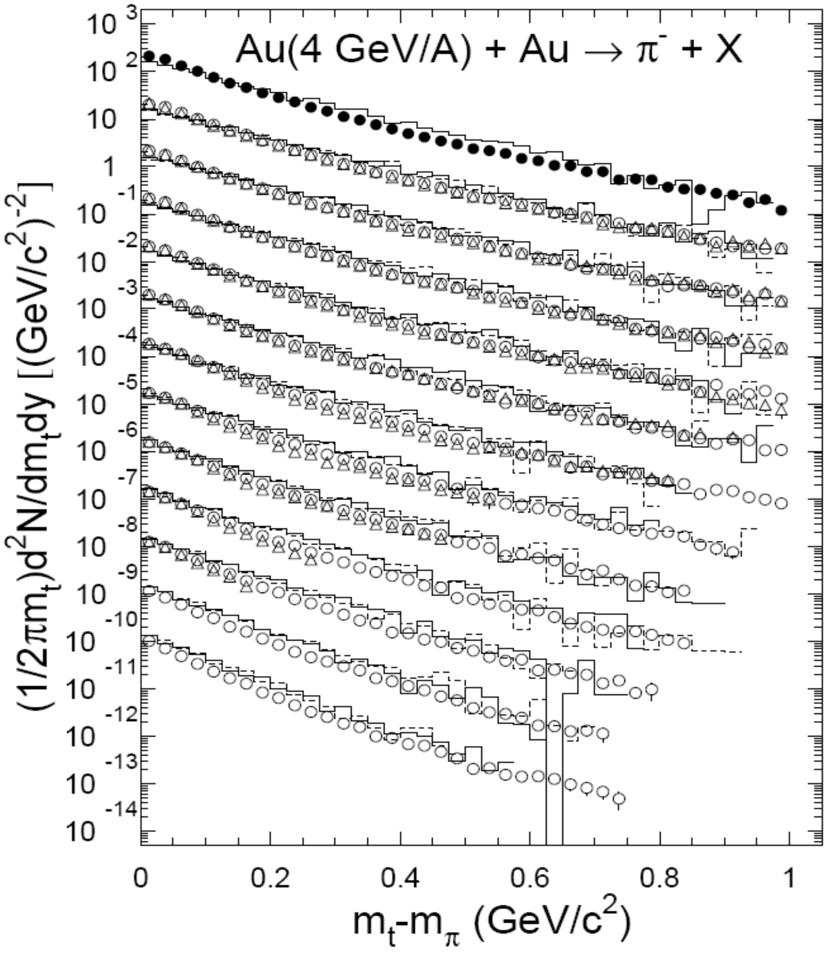

# Nuclear Elastic Scattering

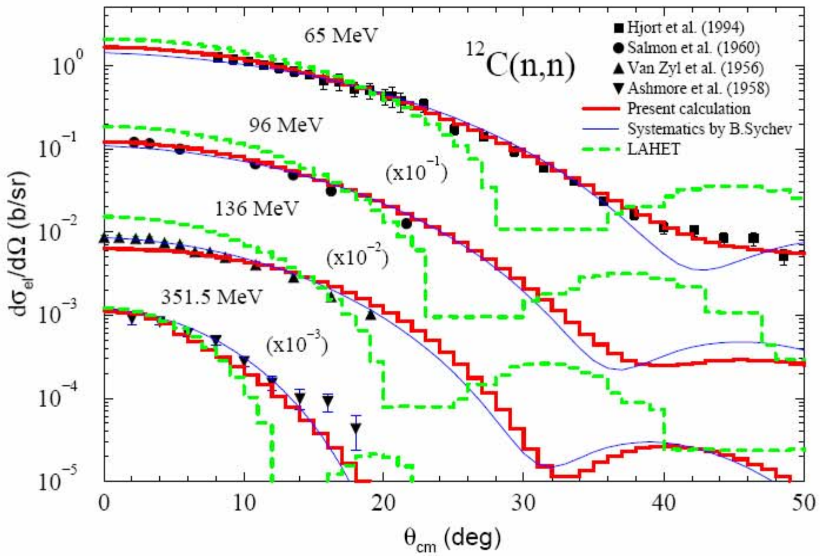


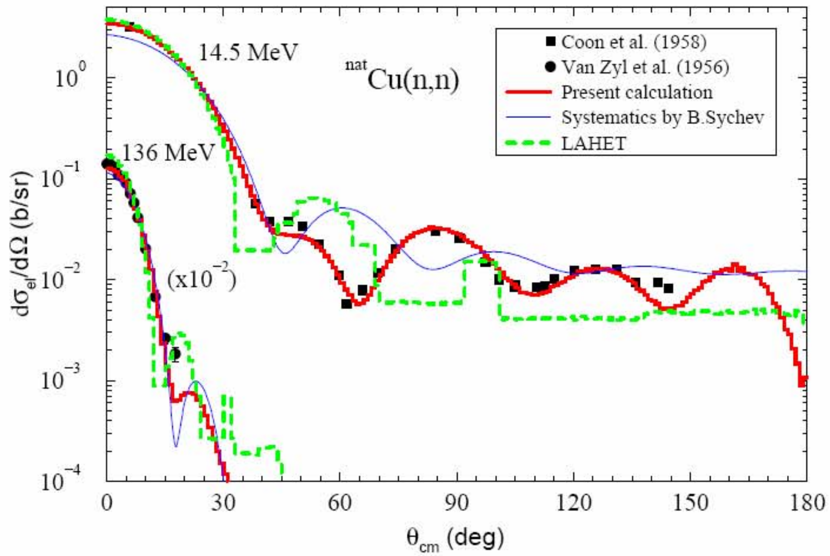


MARS elastic model at E < 5 GeV is based on evaluated data from LA-150, ENDF/HE-VI and Sukhovitski, Chiba et al, supplied with phenomenology where needed. At E > 5 GeV is is a set of phenomenological models.

# Muons, Neutrinos and Stopped Particles

Analog or inclusive simulation algorithms are used for unstable particle decays, prompt muon production (single muons in charmed meson decays, $\mu^+\mu^-$ pairs in vector muon decays, and the dimuon continum), Bethe-Heitler $\mu^+\mu^-$ pairs and direct $e^+e^-$ -> $\mu^+\mu^-$ annihilation.

Neutrinos from meson and muon decays are forced to interact with matter in the following processes:

$$\nu_\mu N \to \mu^+ X, \nu_\mu N \to \nu_\mu X, \nu_\mu p \to \mu^+ n, \nu_\mu p \to \nu_\mu p, \nu_\mu n \to \nu_\mu n,$$
$$\nu_\mu e^- \to \nu_\mu e^-, \nu_\mu e^- \to \nu_e \mu^-, \nu_\mu A \to \nu_\mu A.$$

**Slowing down pion and muon decays and nuclear capture are carefully modeled in a competition. Antiproton annihilation is modeled by LAQGSM or native M15 model.**

# Mean Stopping Power (1)

The mean ionization energy loss for charged particles, except for heavy ions, is calculated using Bethe formalism with the density correction. For heavy ions the Lindhard-Sørensen correction to the regular ionization logarithm and Barkas term are taken into account. In addition, at low ion kinetic energies, the processes of electron capture and loss are accounted for by means of an effective ion charge. The effective charge, $z_{eff}$, is determined according to semi-empirical formulae and used instead of bare ion charge. The remaining discrepancy between theory and experiment observed for heavy target nuclei (about 6% for lead) may require further studies.

# Mean Stopping Power (2)

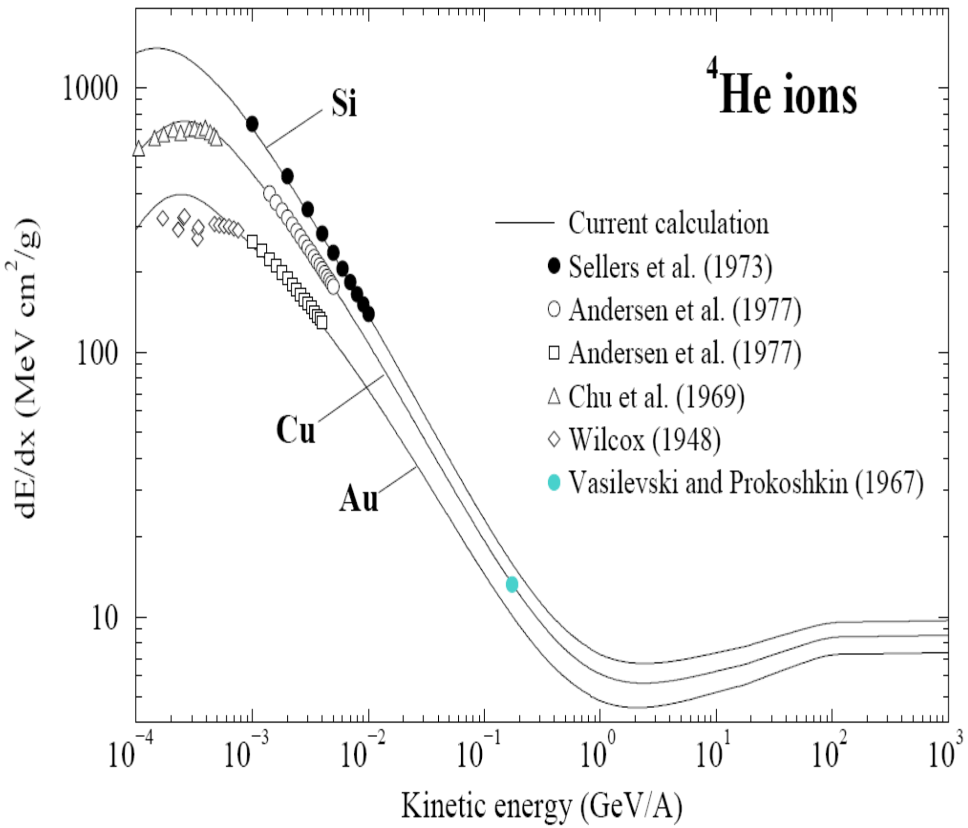


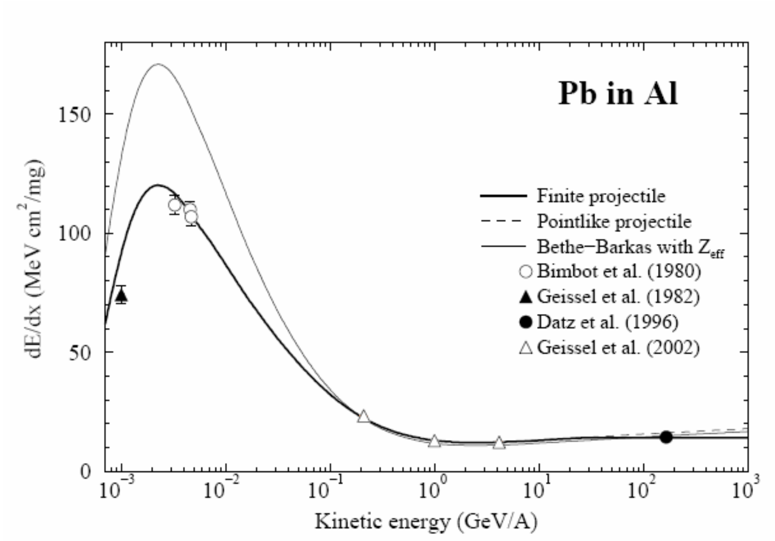


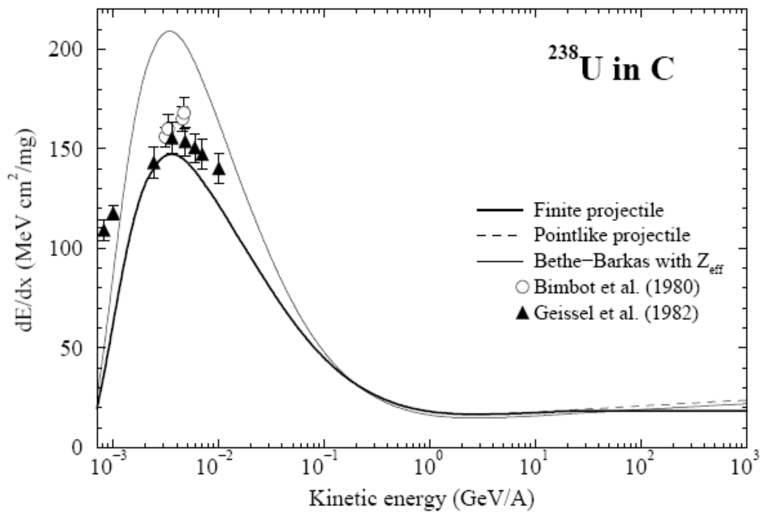

# Correlated Energy Loss and Coulomb Scattering (1)

An efficient method to simulate multiple scattering is based on a separate treatment of "soft" and "hard" interactions. Angular deflection in a large number of "soft" collisions is sampled from a "continues" distribution, "hard" scattering are simulated explicitly. There is an obvious correlation between precision and efficiency of the algorithm and the value of a boundary angle $\theta_b$ between "soft" and "hard" collisions. For small $\theta_b$, a number of discrete interactions is large and precision is high, for larger $\theta_b$, the efficiency increases but the accuracy decreases.

In SAMCS "continues" angular distribution is given by

$$F_c(\theta,t) = \frac{1}{\pi < \theta_s^2 >} e^{-\phi_s} (1 + r_s L_2(\phi_s) + 3r_s^2 L_4(\phi_s) + \ldots),$$

where $\phi_s = \frac{\theta^2}{<\theta_s^2>}$, $r_s = \frac{<\theta_s^4>}{2<\theta_s^2>^2}$, $< \theta^k >= t \int_0^{\theta_b} d\Omega \theta^k \frac{d\Sigma}{d\Omega}$, $L_k$ are Laguerre polynomials.

"Continues" energy loss distribution are described by modified Vavilov distribution. Simulation of "hard" collisions takes into account projectile and nucleus charged distributions and exact kinematics of a projectile-electron interactions.

# Correlated Energy Loss and Coulomb Scattering (2)

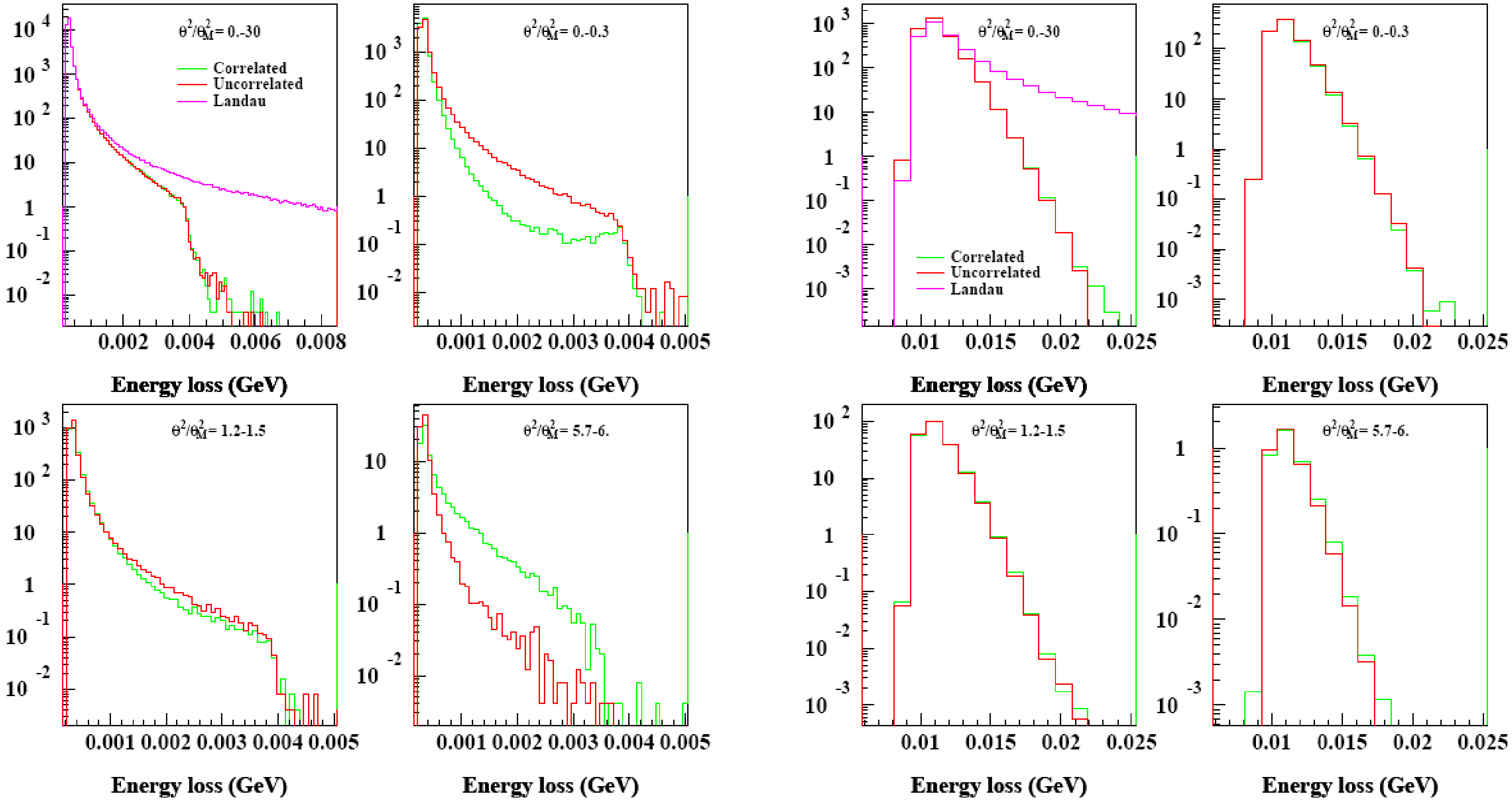


1 cm $LH_2$

30 cm $LH_2$

Energy loss distribution of 200 MeV/c muon

# Coulomb Scattering: Models vs Data

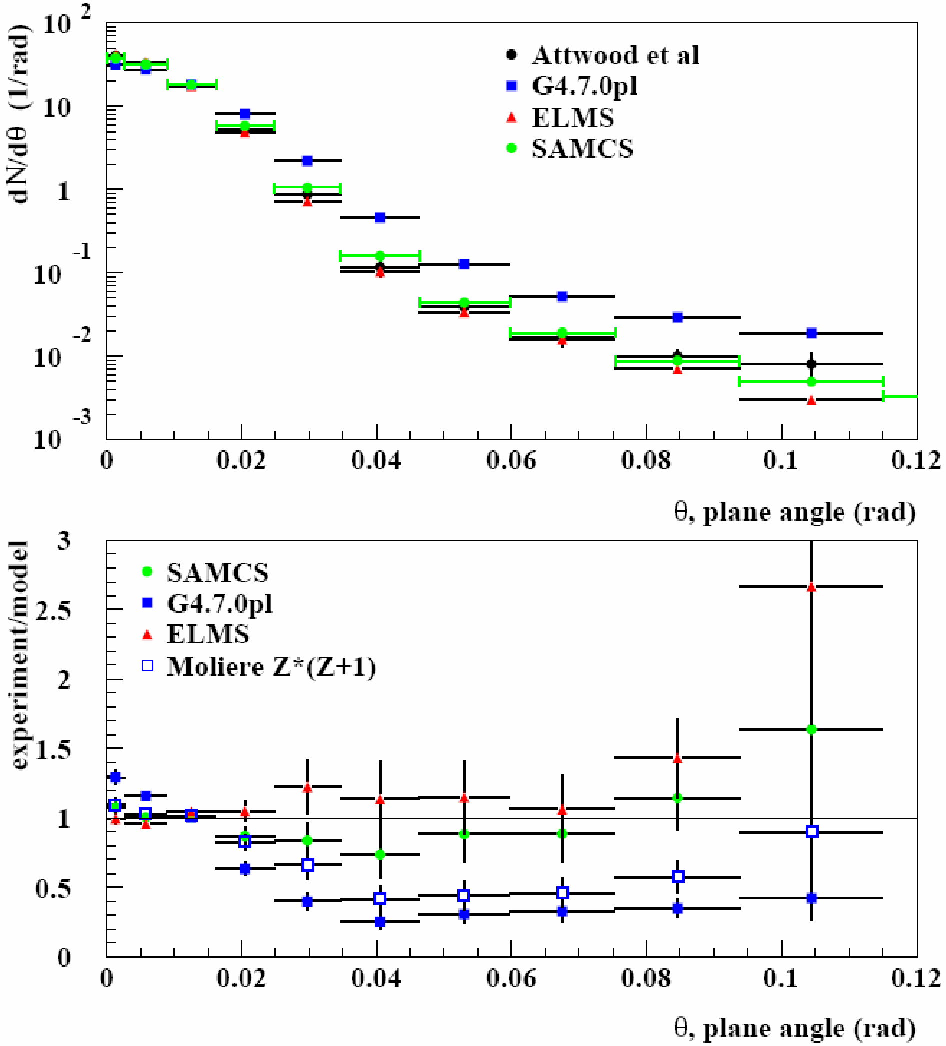


Angular distribution of 172 MeV/c muon after 159 mm of liquid hydrogen

# BIASING

Many processes in MARS15, such as electromagnetic showers, most of hadron-nucleus interactions, decays of unstable particles, emission of synchrotron photons, photohadron production and muon pair production, can be treated either analogously or inclusively with corresponding statistical weights. The choice of method is left for the user to decide, via the input settings.

Other variance reduction techniques used in MARS: weight-window, splitting and Russian roulette, exponential transformation, probability scoring, step/energy cutoffs.

**Goal: Maximize computing efficiency $\varepsilon = t_0/t$, where $t$ is CPU time needed to get a RMS error $\sigma$ equal to the one in the reference method with CPU time $t_0$ provided $\sigma < 20\%$.**

# PHYSICS PROCESS BIAS CONTROL

A user-friendly global bias control was introduced *additionally* via a card **BIAS** with parameters which define exclusive/inclusive switch, Russian Roulette and/or exponential transform control for six processes:

- PPIKDEC- decays of unstable particles
- PMUPRMT -prompt muon production
- PMUBEHE – Bethe-Heitler muon production
- PMUANN – $e^+e^-$ -> $\mu^+\mu^-$ annihillation
- PPHNUC – photo-nuclear reactions
- PPBAR - anti-proton production

# TAGGING

- Further enhanced tagging module in MARS15 allows one to tag the origin of a given signal/tally: geometry, process and phase-space. Invaluable in studying a source term and for sensitivity analysis.

- User-friendly access to process ID at scoring (histograming) stage: flags to 50 process types.

# Origin Tagging in Subroutine TAGPR

```
SUBROUTINE TAGPR(NREG,IM,JJ,W,E1,E2,X,Y,Z,STEP)
C..................................................
*     Origin tagging for hadrons, muons, heavy ions and electromagnetic showers (EMS).
*
*     Particle JJ of weight W and energy E1 makes a step STEP starting from point (X,Y,Z) in region NREG. Both this point and the step fully belong
*     to the region NREG with material index IM. Particle energy at the end of the step is E2. The current history number is NI.
*
*     This particle (JJ is not 9, 10 or 11) or the EMS (JJ is 9, 10 or 11) was originated by particle with ID=IORIG of energy EORIG and weight WORIG in
*     the process KORIG at the point (XORIG,YORIG,ZORIG) in the region NRORIG with material index IMORIG.

*     KORIG = 0 - primary beam
*              1 - muons,   unstable particle decay
*              2 - muons,   prompt at hA-vertex
*              3 - muons,   Bethe-Heitler pair
*              4 - muons,   e+e- annihilation
*              5 - hadrons, hA-vertex
*              6 - hadrons, elastic
*              7 - hadrons, from muons
*              8 - hadrons, unstable particle decay
*              9 - hadrons, EMS
*             10 - hadrons, recoil LEN
*             11 - hadrons, from neutrinos
*             12 - EMS,     induced by photons from pi0-decay
*             13 - EMS,     induced by synchrotron photons
*             14 - EMS,     induced by g,e+,e-, at hA vertex
*             15 - EMS,     induced by knock-on electrons from muons or hadrons
*             16 - EMS,     induced by g,e+,e- from unstable particle decay
*             17 - EMS,     induced by prompt e+e- from muons or hadrons
*             18 - EMS,     induced by brems photons from muon
*             19 - EMS,     induced by photons from stopped muons
*             20 - EMS,     induced by photons from low-energy neutrons
```

# Process ID in Subroutine MFILL

**SUBROUTINE MFILL (IHTYP,NREG,IM,JJ,E1,E2,DELE,W,X1,Y1,Z1,X2,Y2,Z2,DCX,DCY,DCZ,STEP,TOF,NI,IDPRC)**

C 1 DPA ELASTIC AND INELASTIC
C 2 RECOIL NUCLEUS LOCAL DEPOSITION (NON-LAQGSM)
C 3 Local deposition of heavy ions at AA-vertex (NON-LAQGSM)
C 4 STAR DENSITY
C 5 FISSION CEM LOCAL (NON-LAQGSM)
C 6 FISSION >5 GEV LOCAL (NON-LAQGSM)
C 7 HEAVY FRAGMENTS LOCAL DEPOSITION (NON-LAQGSM)
C 8 d, t, He3 and He4 LOCAL DEPOSITION (NON-LAQGSM)
C 9 SURFACE CROSSING BY HADRONS AT IND(6)=T
C 10 STAR DENSITY AT IND(6)=T
C 11 FLUENCE AT IND(6)=T
C 12 ENERGY DEPOSITION by SUB-THRESHOLD hadrons
C 13 SURFACE CROSSING BY NEAR-THRESHOLD HADRONS
C 14 FLUENCE BY NEAR-THRESHOLD HADRONS
C 15 ENERGY DEPOSITION ON STEP BY NEAR-THRESHOLD HADRONS
C 16 SURFACE CROSSING BY NEUTRAL HADRONS OR IN VACUUM
C 17 SURFACE CROSSING BY CHARGED HADRONS IN MATERIAL
C 18 ENERGY DEPOSITION ON STEP BY CHARGED HADRONS
C 19 FLUENCE BY HADRONS
C 20 ENERGY DEPOSITION BY SUB-THRESHOLD e+e- from hadrons
C 21 e+e- vertex by muon
C 22 FLUENCE BY MUONS
C 23 SURFACE CROSSING BY MUONS
C 24 ENERGY DEPOSITION ON STEP BY MUONS
C 25 BREMS VERTEX BY MUONS
C 26 NUCL VERTEX BY MUONS
C 27 ENERGY DEP BY SUB-THRESH BREMS OR NUCL PRODUCTS OF MUONS
C 28 ENERGY DEPOSITION BY SUB-THRESHOLD MUONS
C 29 ENERGY DEPOSITION BY HEAVY FRAGMENTS FROM MUON CAPTURE
C 30 MUON DECAY VERTEX
C 31 SURFACE CROSSING BY EMS
C 32 FLUENCE BY EMS
C 33 ENERGY DEPOSITION ON STEP BY e+ and e-
C 34 ENERGY DEPOSITION BY SUB-THRESHOLD EMS
C 35 DELTA-ELECTRON VERTEX
C 36 LE neutron vertex
C 37 LE NEUTRON FLUENCE ON STEP
C 38 LE NEUTRON SURFACE X-ING
C 39 LE NEUTRON SURFACE CROSSING AT IND(6)=T
C 40 LE NEUTRON FLUENCE AT IND(6)=T
C 41 LE NEUTRON LOCAL ED: no new n or gamma generated
C 42 LE NEUTRON LOCAL ED: recoil proton below 50 keV (E1=Ep)
C 43 LE NEUTRON LOCAL ED: deuteron in non-LAQGSM (E1=Ed)
C 44 LE NEUTRON LOCAL ED: vertex non-fission MCNP (E1=Eterm)
C 45 LE NEUTRON LOCAL ED: capture on Li or B in non-LAQGSM (E1=Ehi)
C 46 LE NEUTRON LOCAL ED: sub-threshold (E1=En)
C 47 LE NEUTRON LOCAL ED: SUB-THRESHOLD AT IND(6)=T
C 48 LE NEUTRON LOCAL ED: fission
C 49 LE NEUTRON LOCAL ED: vertex non-fission BNAB
C 50 FLUENCE BY NEUTRINO

# GEOMETRY DESCRIPTIONS IN MARS15

***Five geometry description options***

1. **Standard**: heterogeneous *R-Z-Φ* cylinder.
2. **Non-standard**: arbitrary user-defined in Fortran or C.
3. **Extended**: a set of contiguous or overlapping geometrical shapes, currently, boxes, spheres, cylinders, truncated cones, tetrahedra, and elliptical tubes. Can be subdivided into many sub-regions in each direction; arbitrary transformation matrices can be applied to any object.
4. **MCNP**: read in an input geometry description in the MCNP format.
5. **FLUKA**: read in an input geometry description in the FLUKA format.

# GEOMETRIES AND MATERIALS

Only extended geometry option provides exact crossing of particle tracks with surfaces that prevents small regions within a large volume from being skipped over. In other four options, boundary localization is based on iterative algorithm and user needs to take care of appropriate region numbering, pilot steps and localization parameters.

All five geometry options can co-exist in a setup description. Arbitrary number of regions, with a default of $10^5$. Volumes of all regions are auto-calculated for the predefined shapes or using a short session of the program. A corresponding output file provides calculated volumes with statistical errors, and is directly linked to the main code.

A list of built-in materials include 165 ones. Added many kinds of steel, cast iron, mineral oil, gadalinium-loaded scintillator, etc. User-defined composite option on top of that is kept. Separate treatment of gaseous and liquid states.

# SIMPLE GEO EXAMPLE: GEOM.INP

```
 Extended Demo  05/17/06
OPT
box-1      1 0 2   0.  -5.   5.  10.  10. 15. 1 4 3
cyl-1a    -2 1 7   0.   0.   0.   0.   5. 20.
cyl-1a    -2 1 1   0.   0.   0.   5.  10. 20. 4 2
ball-a     3 0 8   0.   25. 20.   0.   5.
ball-b     3 0 3   0.   25. 20.   5.  10. 3
cone-in   -4 0 0   0. -30.  30.   0.   3.  0.  6. 20.
cone-out  -4 0 4   0. -30.  30.   3.   5.  6. 12. 20. 2 2
th         5 0 6   0. 0. 35. 5. 3. 55. 0. 20. 60. 0. -5. 65.
ell-tub1  -6 2 6   0.   0.   0.   8.   3.  0.  40.
ell-tub2  -6 2 5   0.   0.   0.   8.   3.  3.  40.
TR1  0.  -15. 75. -20.
TR2  0.   30. 70.  20. 90.
stop
```

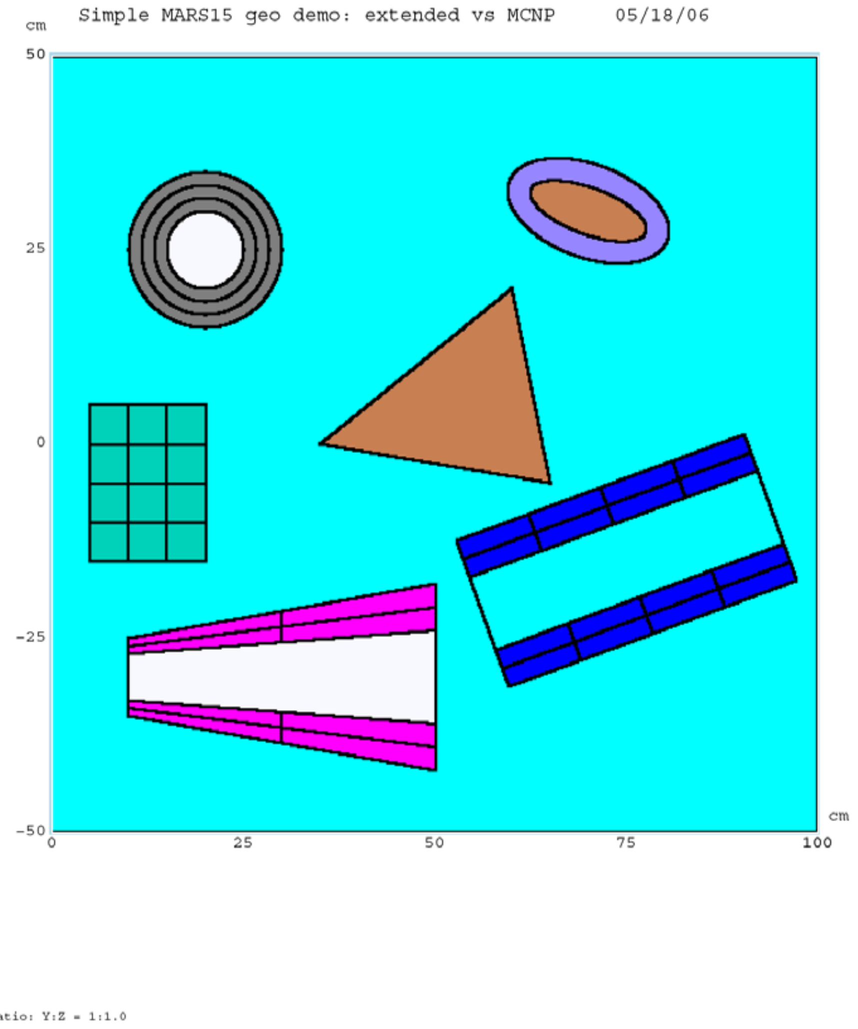

# SAME EXAMPLE: MARS.INP with MCNP Geometry

```
 Extended & MCNP Demo  05/17/06
/home/mokhov/restricted/mars15/dat
INDX 3=F 5=T 16=T
CTRL 1
NEVT 50
ENRG 10.
ZSEC 100.
RSEC 50. 101=7
NMAT 7
MATR 'NBS2' 'SCI' 'CONC' 'MRBL' 'CAST' 'S316' 'AIR'
NHBK 1
STOP
*MCNP START
1  7  -0.00129     2 -1   (-26:27:25)    8 17 (-19:21:23) imp:n,p=1
2  2  -0.7903      -2     -3    -6              imp:n,p=1
3  2  -0.7903      -2    3 -4    -6             imp:n,p=1
4  2  -0.7903      -2    4 -5    -6             imp:n,p=1
5  2  -0.7903      -2    5       -6             imp:n,p=1
6  2  -0.7903      -2     -3   6 -7             imp:n,p=1
7  2  -0.7903      -2    3 -4   6 -7            imp:n,p=1
8  2  -0.7903      -2    4 -5   6 -7            imp:n,p=1
9  2  -0.7903      -2    5      6 -7            imp:n,p=1
10  2  -0.7903      -2     -3   7               imp:n,p=1
11  2  -0.7903      -2    3 -4   7              imp:n,p=1
12  2  -0.7903      -2    4 -5   7              imp:n,p=1
13  2  -0.7903      -2    5      7              imp:n,p=1
14  7  -0.00129      -8    -9                   imp:n,p=1
15  1  -7.0        -8  9 -10     -11            imp:n,p=1
16  1  -7.0        -8  9 -10   11 -12           imp:n,p=1
17  1  -7.0        -8  9 -10   12 -13           imp:n,p=1
18  1  -7.0        -8  9 -10   13               imp:n,p=1
19  1  -7.0        -8 10        -11             imp:n,p=1
20  1  -7.0        -8 10      11 -12            imp:n,p=1
21  1  -7.0        -8 10      12 -13            imp:n,p=1
22  1  -7.0        -8 10      13                imp:n,p=1
23  0              -14                          imp:n,p=1
24  3  -2.35       14 -15                       imp:n,p=1
25  3  -2.35       15 -16                       imp:n,p=1
26  3  -2.35       16 -17                       imp:n,p=1
27  0              -18   19 -21                 imp:n,p=1
28  4  -2.7        18 -22   19 -20              imp:n,p=1
29  4  -2.7        18 -22   20 -21              imp:n,p=1
30  4  -2.7        22 -23   19 -20              imp:n,p=1
31  4  -2.7        22 -23   20 -21              imp:n,p=1
32  6  -7.92          -24   26 -27              imp:n,p=1
33  5  -7.31       24 -25   26 -27              imp:n,p=1
34  0              1                            imp:n,p=0
1    rcc     0 0 0     0 0 100     50
2    rpp    -10 10    -15 5     5 20
3    py   -10
4    py    -5
5    py     0
6    pz    10
7    pz    15
8  1  rcc     0 0 -20    0 0 40    10
9  1  cz     5
10 1  cz     7.5
11 1  pz   -10
12 1  pz     0
13 1  pz    10
14    s     0 25 20    5
15    s     0 25 20    6.667
16    s     0 25 20    8.333
17    s     0 25 20   10
18   k/z   0 -30 -30   .005625
19   pz     10
20   pz     30
21   pz     50
22   k/z   0 -30 -22      .015625
23   k/z   0 -30 -18.57   .030626
24 2 sq    0  64  9   0 0 0  -576   0 0 0
25 2 sq    0 121 36   0 0 0 -4356   0 0 0
26   px  -40
27   px   40
mode n p

m1   2004 -.02    29000 -.38    13027 -.2     41093 -.280522     50000 -.119478   $  NBS2
m2   1001 -.13314  6000 -.86651  7014 -.00016   8016 -.00019             $  SCI
m3   1001 -.006    6000 -.030    8016 -.500    11023 -.010 13027 -0.03 &  $  Conc
   14000 -.200   19000 -.010   20000 -.200    26000.42c -.014
m4  20000 -.400431 6000 -.120005 8016 -.479564                     $  MRBL
m5   6000 -.0365  14000 -.025   25055 -.0018   26000.42c -.9347  29000 -.002 $ CAST
m6  24000 -.17    25055 -.02   26000.42c -.655 28000  -.12  14000 -.01   42000 -.025 $ S316
m7   7014  .78443  8016  .21076 18000.42c 4.671E-3 6000 1.39E-4 gas=1      $  Air
vol  1 33r
*MCNP END
```

# CMS Detector in MARS15 with FLUKA Input

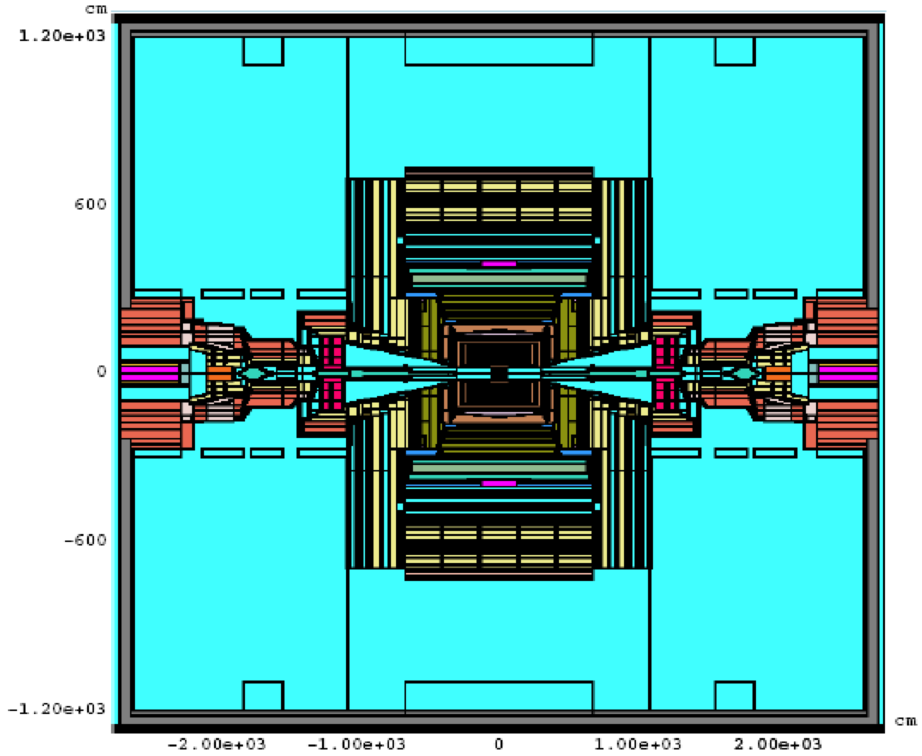


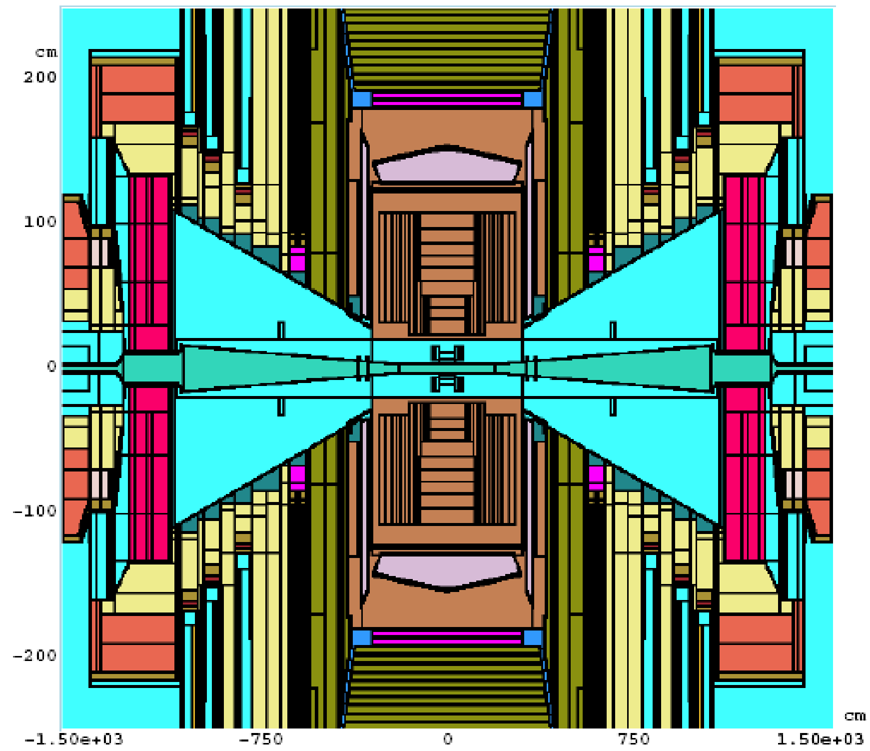


CMS detector in MARS15

# TRACKING & HISTOGRAMING

Tracking - in magnetic field with Coulomb scattering and energy loss for charged particles - and histograming algorithms are quite sophisticated to assure highest accuracy and CPU performance.

User-friendly flexible XYZ-histograming module allows scoring numerous distributions – total and partial particle fluxes, star density, energy deposition, DPA, temperature rise, prompt and residual dose rates, particle spectra etc – in boxes arbitrary positioned in a 3D system, independent of geometry description. Detailed nuclide inventory.

# GRAPHICAL-USER INTERFACE

The existing Tcl/Tk-based 2D MARS-GUI-SLICE functionality was further improved and extended to 3D, which further extends the power of visualization of the modeled system: geometry, materials and magnetic field descriptions, simulated processes and calculated results. Arbitrary 3-D rotation of a slice is possible. The new module in MARS15 is based on the Open Inventor graphics library, integrated with MARS-GUI-SLICE. It has also been re-implemented using the C++ based Qt-toolkit. The new 3D display capability was developed using open source libraries that should allow redistribution of the code and/or binaries to the MARS user community, free of commercial licensing terms.

# MARS MODELING OF CDF DETECTOR

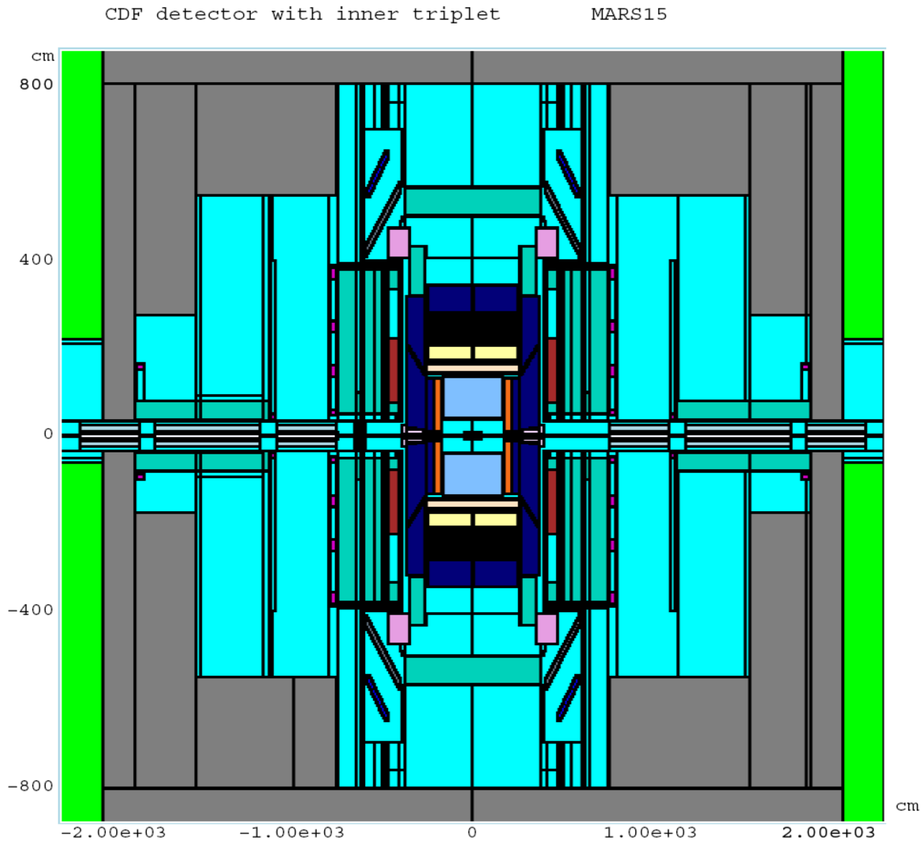


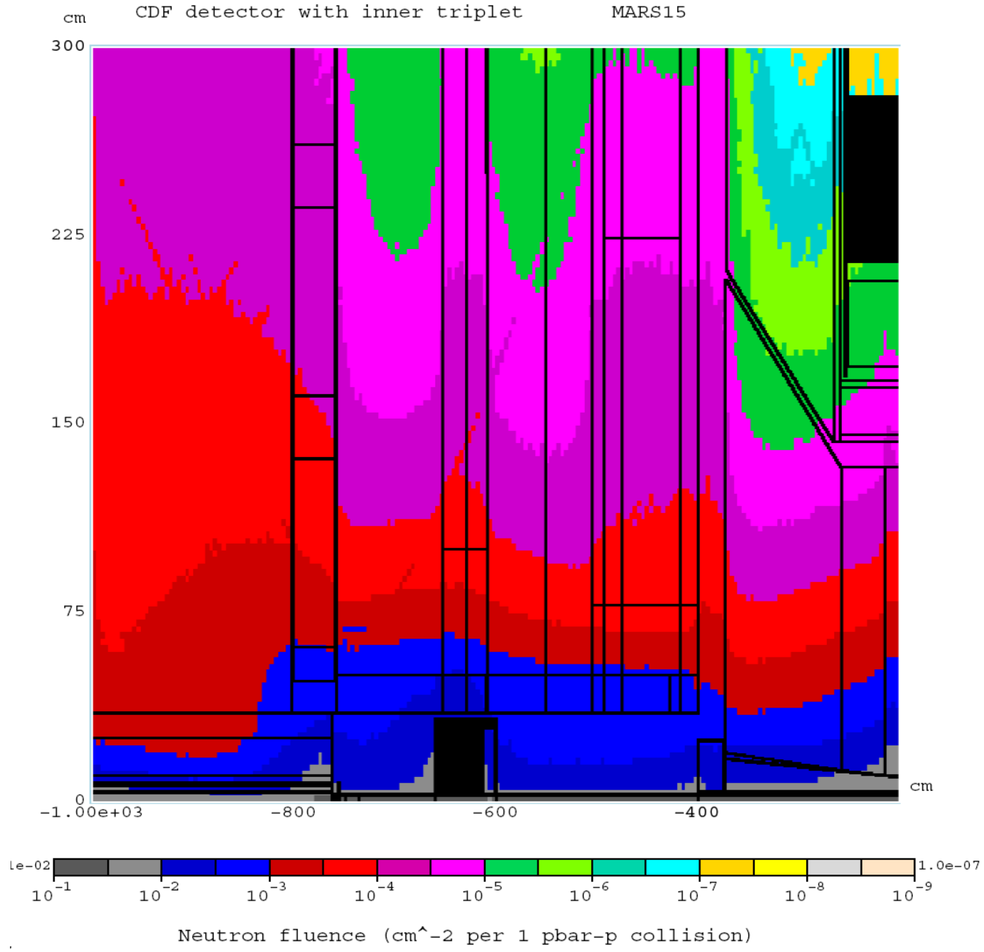


CDF detector, experimental hall, Tevatron beamline elements and neutron fluence isocontours as seen in MARS15 GUI

# MAD-MARS BEAM LINE BUILDER

The interface system to build beam line and accelerator models in the MARS format. MMBLB reads in a MAD lattice file and puts the elements in the same order into MARS. Each element is assigned six functions: element type/name, geometry, materials, field, volume and initialization. MMBLB has been substantially extended for MARS15:

- The set of supported element types includes now almost all the elements supported by MAD.
- An arbitrary number of beam lines – arbitrary positioned and oriented – can be put in a MARS15 model.
- More sophisticated algorithms and new data structures enable more efficient searches through the beam line geometry.
- Tunnel geometry can now follow the beam line or be described independently of it.

# MMBLB for 500-m LHC IP5

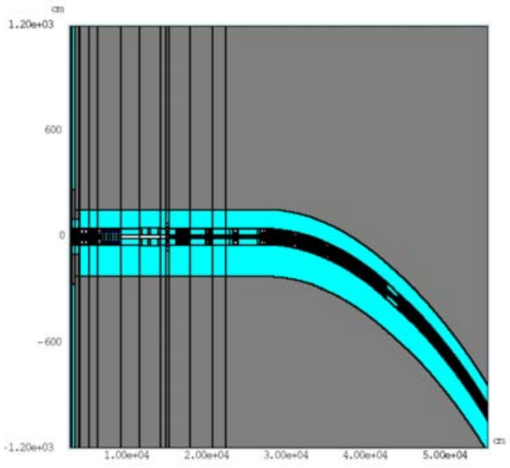


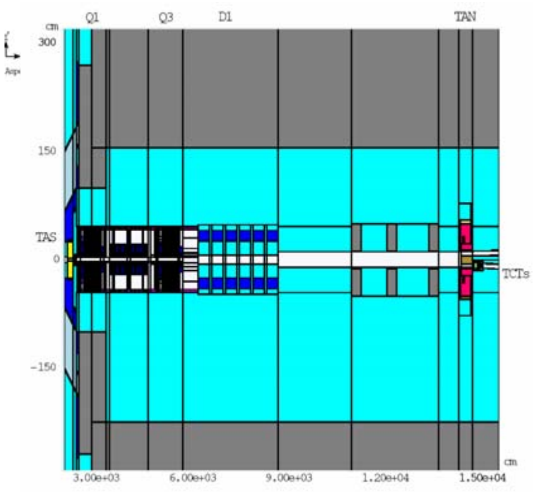


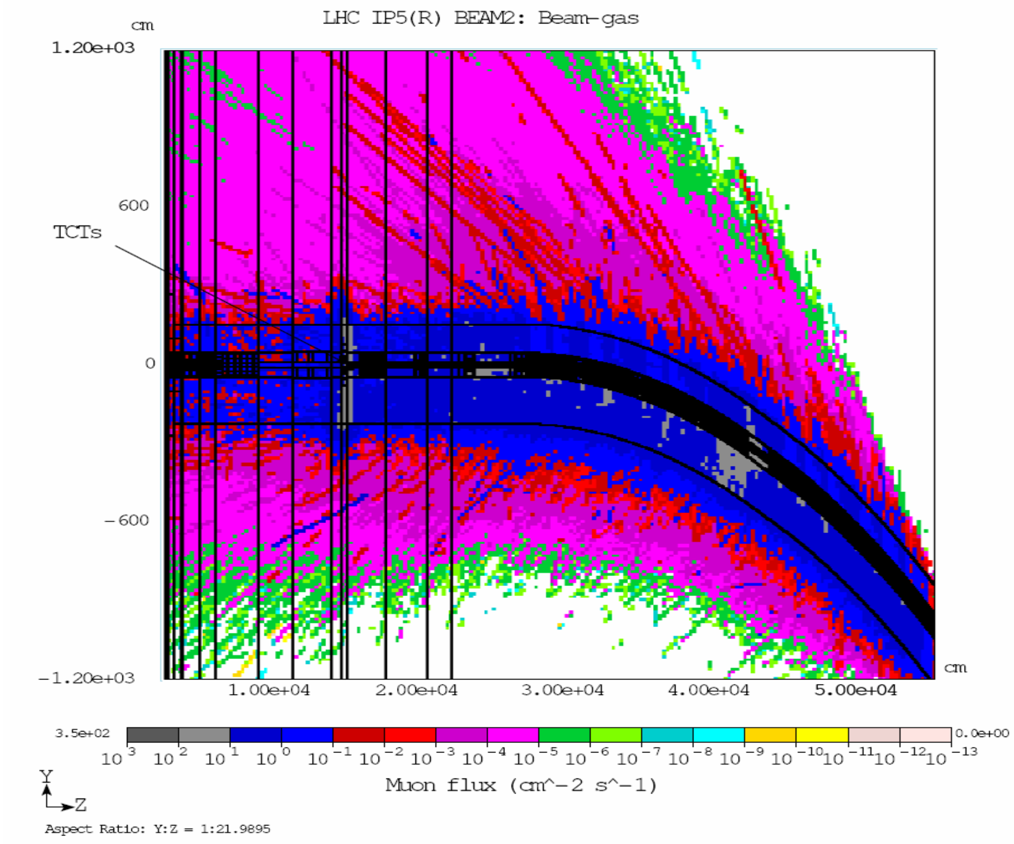


Kilometers of magnetic structure with detailed 3D geometry in Tevatron, LHC and ILC; entire ring description for J-PARC and Fermilab Booster

# MULTIPROCESSING IN MARS15

Since 2004, parallel processing is default in all CPU-hungry applications of MARS15. It is based on the Message Passing Interface(MPI) libraries. Parallelization is job-based, i.e. the processes, replicating the same geometry of the setup studied, run independently with different initial seeds. A unique master process -- also running event histories -- collects intermediate results from an arbitrary number of slaves and calculates the final results when a required total number of events has been processed. Intermediate results are sent to the master on its request generated in accordance with a scheduling mechanism. The performance scales almost linearly with the number of nodes used (up to tens of nodes at Fermilab clusters).

# A FEW RECENT MARS15 APPLICATIONS AT FERMILAB

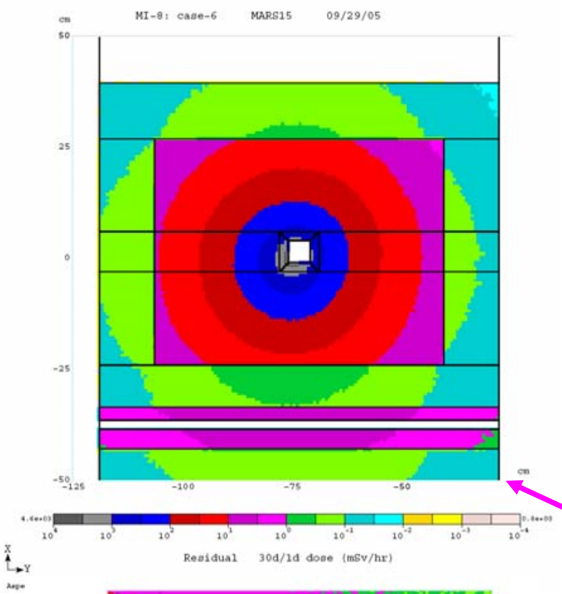


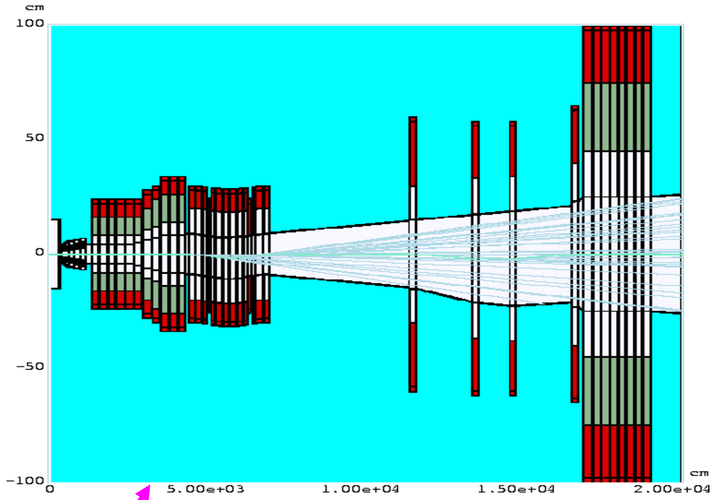

SNuMI: 1.2-MW beam, marble in collimators

ILC: Collimation, detectors, 18-MW beam extraction

MERIT: 26-GeV mercury-jet expt at CERN

LHC: Machine-detector interface, SC magnets, IR upgrades, collimators, forward detectors

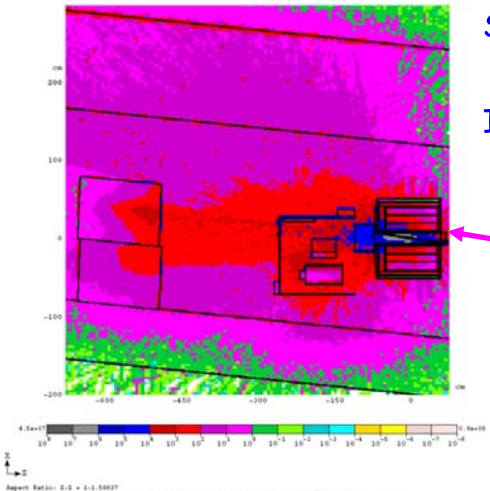

Absorbed dose in Gy/3 · $10^{15}$ protons.

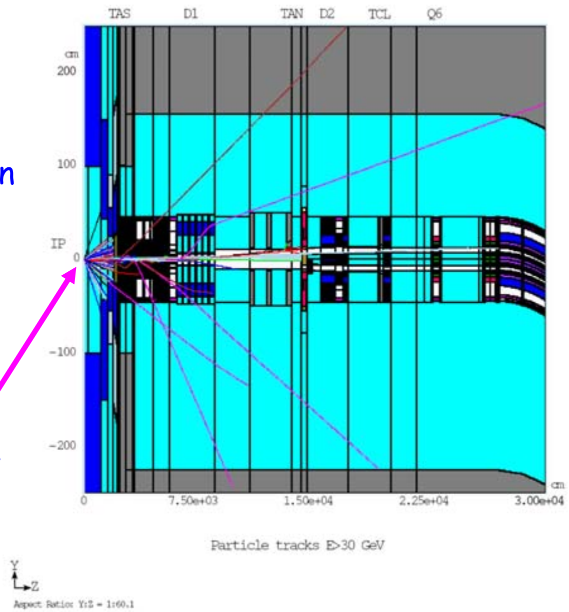

# IP & 2-km BDS Backgrounds in ILC SiD

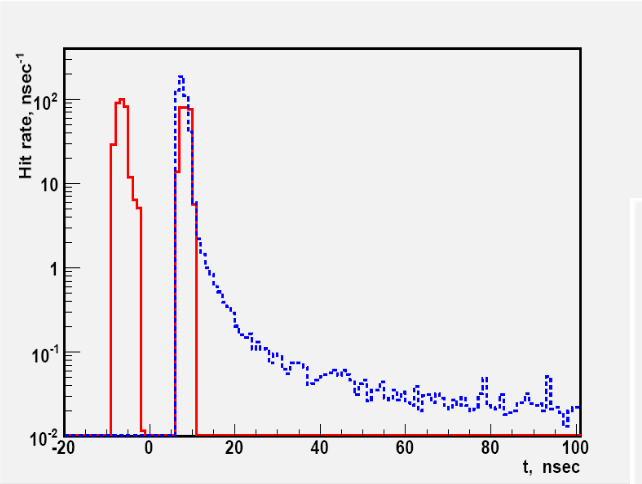


Figure 15: Time distribution of hit rates in Hcal Endcap. Solid line - background (no spoilers), dashed lin $e^+e^-$ events. Background is created by particles coming from positron tunnel only.

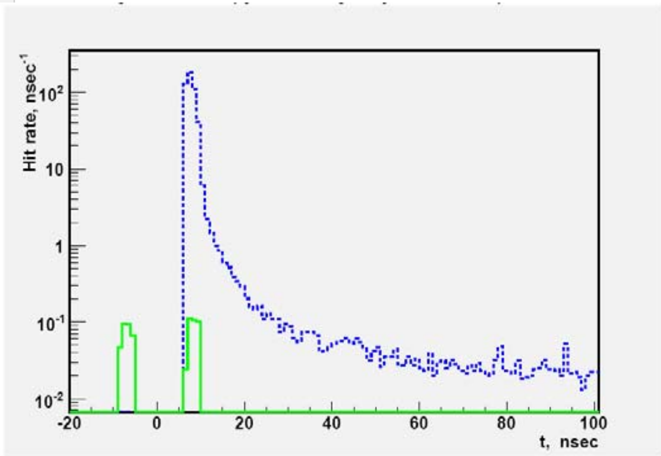


Figure 16: Time distribution of hit rates in Hcal Endcap. Solid line - background (with spoilers), dashed line - $e^+e^-$ events. Background is created by particles coming from positron tunnel only.

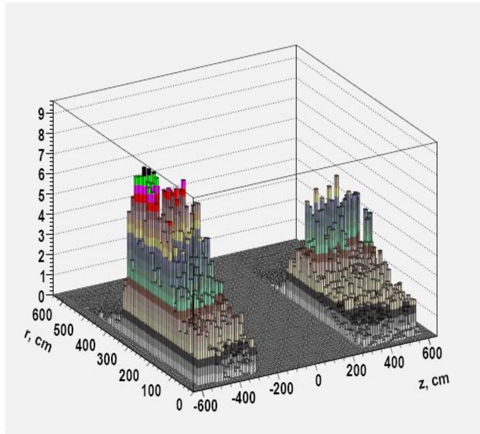


Figure 7: RZ distribution of hits per bunch in Muon Endcap. No spoilers. Background is created by particles coming from positron tunnel only.

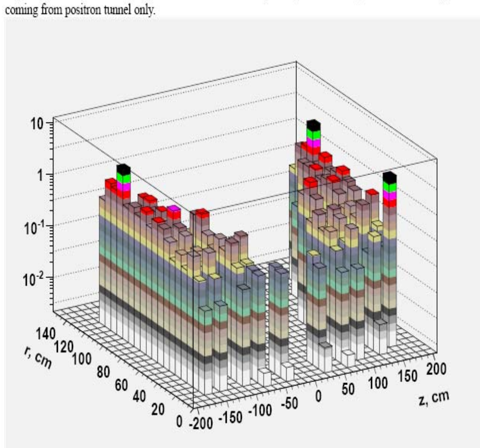


Figure 8: RZ distribution of hits per bunch in Tracker Endcap. No spoilers. Background is created by particles coming from positron tunnel only.

*HCAL Endcap hit rates:*

Red – BDS (no spoilers)
Green – BDS (w/spoilers)
Blue – $e^+e^-$ events

STRUCT+MARS15+SLIC+LCDD+PYTHIA